Neurobiology of Disease 125 (2019) 176–189

Contents lists available at ScienceDirect

Neurobiology of Disease

journal homepage: www.elsevier.com/locate/ynbdi

Loss of biliverdin reductase-A favors Tau hyper-phosphorylation in Alzheimer's disease

Nidhi Sharma[a], Antonella Tramutola[a], Chiara Lanzillotta[a], Andrea Arena[a], Carla Blarzino[a], Tommaso Cassano[b], D. Allan Butterfield[c], Fabio Di Domenico[a], Marzia Perluigi[a], Eugenio Barone[a,*]

[a] Department of Biochemical Sciences "A. Rossi-Fanelli", Sapienza University of Rome, Piazzale A. Moro 5, Roma 00185, Italy
[b] Department of Clinical and Experimental Medicine, University of Foggia, Via L. Pinto, Foggia 71122, Italy
[c] Department of Chemistry, Markey Cancer Center, and Sanders-Brown Center on Aging, University of Kentucky, Lexington, KY 40506-0055, USA

ARTICLE INFO

Keywords:
Alzheimer's disease
Akt
Biliverdin reductase-A
GSK-3β
Oxidative stress
Tau phosphorylation

ABSTRACT

Hyper-active GSK-3β favors Tau phosphorylation during the progression of Alzheimer's disease (AD). Akt is one of the main kinases inhibiting GSK-3β and its activation occurs in response to neurotoxic stimuli including, i.e., oxidative stress. Biliverdin reductase-A (BVR-A) is a scaffold protein favoring the Akt-mediated inhibition of GSK-3β. Reduced BVR-A levels along with increased oxidative stress were observed early in the hippocampus of 3xTg-AD mice (at 6 months), thus suggesting that loss of BVR-A could be a limiting factor in the oxidative stress-induced Akt-mediated inhibition of GSK-3β in AD.

We evaluated changes of BVR-A, Akt, GSK-3β, oxidative stress and Tau phosphorylation levels: (a) in brain from young (6-months) and old (12-months) 3xTg-AD mice; and (b) in post-mortem inferior parietal lobule (IPL) samples from amnestic mild cognitive impairment (MCI), from AD and from age-matched controls. Furthermore, similar analyses were performed in vitro in cells lacking BVR-A and treated with H_2O_2.

Reduced BVR-A levels along with: (a) increased oxidative stress; (b) reduced GSK-3β inhibition; and (c) increased Tau Ser404 phosphorylation (target of GSK-3β activity) without changes of Akt activation in young mice, were observed. Similar findings were obtained in MCI, consistent with the notion that this is a molecular mechanism disrupted in humans. Interestingly, cells lacking BVR-A and treated with H_2O_2 showed reduced GSK-3β inhibition and increased Tau Ser404 phosphorylation, which resulted from a defect of Akt and GSK-3β physical interaction. Reduced levels of Akt/GSK-3β complex were confirmed in both young 3xTg-AD and MCI brain.

We demonstrated that loss of BVR-A impairs the neuroprotective Akt-mediated inhibition of GSK-3β in response to oxidative stress, thus contributing to Tau hyper-phosphorylation in early stage AD. Such changes potential provide promising therapeutic targets for this devastating disorder.

1. Introduction

Tau, a microtubule-associated protein, has an important role in microtubule assembly and stabilization (Lee et al., 2001; Wang and Mandelkow, 2016) as well as in the regulation of neuronal intracellular trafficking (Dixit et al., 2008; Vershinin et al., 2007). Unfolded Tau shows little tendency for aggregation, but aggregation of hyper-phosphorylated Tau into paired helical filaments (PHFs) and neurofibrillary tangles (NFTs) characterizes a wide range of neurodegenerative diseases known as tauopathies, including Alzheimer's disease (AD) (Griffin et al., 2005; Lebouvier et al., 2017; Lee et al., 2001).

Although the neurotoxic role of Tau aggregates has been confirmed in several studies, both in vitro and in vivo [reviewed in (Congdon and Sigurdsson, 2018; Wang and Mandelkow, 2016)], the mechanisms by which Tau forms aggregates in AD brain, and the pathways underlying Tau-induced neurodegeneration are not completely understood. Protein post-translational modifications including hyper-phosphorylation, acetylation, N-glycosylation and truncation among others, may affect Tau aggregation in several ways (Congdon and Sigurdsson, 2018; Wang and Mandelkow, 2016). Notably, since aggregated Tau in patients with a tauopathy or in transgenic mice invariably show hyper-phosphorylation, and Tau hyper-phosphorylation precedes aggregation,

* Corresponding author at: Department of Biochemical Sciences "A. Rossi-Fanelli", Sapienza University of Rome, Piazzale A. Moro 5, Rome 00185, Italy.
E-mail address: eugenio.barone@uniroma1.it (E. Barone).

https://doi.org/10.1016/j.nbd.2019.02.003
Received 13 December 2018; Received in revised form 31 January 2019; Accepted 4 February 2019
Available online 06 February 2019
0969-9961/

phosphorylation has been assumed to drive Tau aggregation (Wang and Mandelkow, 2016).

Among the kinases identified to be responsible for Tau hyper-phosphorylation, glycogen synthase kinase (GSK)-3β plays an important role in the pathological changes of Tau protein in AD(Medina et al., 2011; Pei et al., 1999). GSK-3β is a ubiquitously expressed serine/threonine kinase active under basal conditions and inactivated upon phosphorylation by different upstream kinases(Krishnankutty et al., 2017; Zhang et al., 2018). In particular, autophosphorylation at Tyr216 promotes GSK-3β activation (Cole et al., 2004; Hughes et al., 1993; Krishnankutty et al., 2017; Lochhead et al., 2006), while phosphorylation at the N-terminal Ser9 is responsible for GSK-3β inhibition (Doble, 2003; Frame and Cohen, 2001; Jensen et al., 2007; Jope and Johnson, 2004; Krishnankutty et al., 2017; Sutherland et al., 1993).

GSK-3β is target of several kinases, i.e., protein kinase A (PKA), members of the mitogen-activated protein kinases (MAPK) family and the ribosomal protein S6 kinase (S6K) (Doble, 2003; Frame and Cohen, 2001; Jensen et al., 2007; Jope and Johnson, 2004; Krishnankutty et al., 2017; Sutherland et al., 1993). However, Akt is the main kinase, which inhibits GSK-3β in response to growth factors and especially insulin (Hermida et al., 2017). Furthermore, Akt-mediated inhibition of GSK-3β represents a neuro-protective and pro-survival mechanism rapidly activated in response to oxidative stress (Chong et al., 2005).

Both oxidative stress and reduced insulin signalling activation in the brain (known as brain insulin resistance), were proposed to favor Tau hyper-phosphorylation in AD (Bomfim et al., 2012; Butterfield et al., 2014; Morales-Corraliza et al., 2016; Rivera et al., 2005; Sajan et al., 2016; Steen et al., 2005; Talbot et al., 2012; van der Harg et al., 2017; Yarchoan et al., 2014; Zhang et al., 2016), although the molecular mechanisms are still unclear.

Data collected in humans show increased activation of GSK-3β in early stage AD (Nicolia et al., 2017), while a consistent inhibition was observed in late stage AD (Griffin et al., 2005; Pei et al., 2003; Tramutola et al., 2015; Yarchoan et al., 2014), thus suggesting that GSK-3β-mediated Tau phosphorylation is among the earliest events during the progression of the pathology. While increased Akt activation was associated with GSK-3β inhibition in late AD (Griffin et al., 2005; Pei et al., 2003; Tramutola et al., 2015; Yarchoan et al., 2014), to our knowledge no data are available for early stage AD (Nicolia et al., 2017).

In searching for the mechanisms responsible for the onset and progression of brain insulin resistance in AD, we focused on the role of biliverdin reductase-A (BVR-A) (Barone et al., 2016; Barone et al., 2011a; Barone et al., 2011b; Barone et al., 2014; Barone et al., 2012; Barone et al., 2018; Di Domenico et al., 2013; Triani et al., 2018). BVR-A – mainly known for its canonical activity in the degradation pathway of heme – is also a unique serine/threonine/tyrosine (Ser/Thr/Tyr) kinase involved in the regulation of insulin signalling (Gibbs et al., 2014; Lerner-Marmarosh et al., 2005). BVR-A is a direct target of the insulin receptor (IR) kinase activity, similar to the insulin receptor substrate-1 (IRS1). IR phosphorylates BVR-A on specific Tyr residues resulting in the activation of BVR-A kinase activity (Lerner-Marmarosh et al., 2005). In turn, once IR-activated, BVR-A phosphorylates IRS1 on inhibitory Ser residues, that represents a mechanism to maintain the correct activation of IRS1 (Lerner-Marmarosh et al., 2005).

Intriguingly, BVR-A – independently of the kinase activity – can function as a scaffold protein, since it contains several sequence motifs identified as protein–protein interaction sites (Kapitulnik and Maines, 2009). In particular, BVR-A markedly increases the activation of Akt, which results in GSK-3β inhibition in vitro (Miralem et al., 2016).

In a previous study from our group we demonstrated age-associated changes of BVR-A in the hippocampus of 3xTg-AD mice (Barone et al., 2016). In particular, we found that decreased BVR-A protein levels and activation occur early in 3xTg-AD mice brain before consistent elevation of AD pathological features (Barone et al., 2016). Reduced BVR-A activation was associated with alterations of the insulin signalling cascade characterized by an initial hyper-activation of IRS1 (at 6 months) followed by IRS1 inhibition later (at 12 and 18 months) (Barone et al., 2016). These changes were also associated with increased oxidative stress.

In young mice, despite increased oxidative stress and hyper-active IRS1, we did not observe a parallel increase of Akt activation (Barone et al., 2016; Barone et al., 2018); however, increased Tau phosphorylation was evident (Barone et al., 2016; Barone et al., 2018).

Therefore, in light of the proposed role for BVR-A in promoting Akt-mediated inhibition of GSK-3β, we hypothesized that a reduction of BVR-A impedes the activation of Akt and the consequent inhibition of GSK-3β under oxidative stress conditions, possibly resulting in Tau hyper-phosphorylation. The results of this study are reported in the present manuscript.

2. Materials and methods

2.1. Animals

Six- and 12-month-old 3 × Tg-AD male mice ($n = 6$ per group) and their male littermates Non-Tg (n = 6 per group) were used in this study. As previously reported by our group, other than the alterations cited above regarding BVR-A and Akt activation in the hippocampus, 3xTg-AD mice are characterized by cognitive dysfunctions evaluated through the Morris water maze and novel object recognition tasks both at 6 and 12 months of age (Barone et al., 2018). Therefore, 6 and 12 months of age are suitable time points to evaluate molecular alterations, which can be associated with functional alterations. The 3 × Tg-AD mice harbour 3 mutant human genes (APP_{Swe}, $PS1_{M146V}$, and Tau_{P301L}) and have been genetically engineered by LaFerla and colleagues (Cassano et al., 2011; Cassano et al., 2012; Oddo et al., 2003). Colonies of 3 × Tg-AD and WT mice were established at the vivarium of Puglia and Basilicata Experimental Zooprophylactic Institute (Foggia, Italy). The housing conditions were controlled (temperature 22 °C, light from 07:00–19:00, humidity 50%–60%), and fresh food and water were freely available. All the experiments were performed in strict compliance with the Italian National Laws (DL 116/92), the European Communities Council Directives (86/609/EEC). All efforts were made to minimize the number of animals used in the study and their suffering. Animals were sacrificed at the selected age and the hippocampi were extracted, flash-frozen, and stored at −80 °C until total protein extraction and further analyses were performed.

2.2. Human samples

Brain tissues from well characterized subjects were provided by Sanders-Brown Center on Aging of the University of Kentucky. All the studies were performed on the inferior parietal lobule (IPL) of non-disease control, MCI or AD cases. Clinical diagnosis of disease stage was made as described previously (Aluise et al., 2010; Aluise et al., 2011). Age and gender are listed in the Table 1. The short post-mortem interval range was between 2 and 4 h and was comparable between the three groups. The degree of cognitive impairment was assessed using the Mini Mental State Examination (MMSE) (and listed in Table 1).

2.3. Cell culture and treatments

The HEK cells were grown in Dulbecco's modified Eagle's medium (DMEM) high glucose (25 mM) supplemented with 10% fetal bovine serum (FBS), 2 mM L-glutamine, penicillin (20 units/mL) and streptomycin (20 mg/mL), (GIBCO, Gaithersburg, MD, U.S.A.). Cells were maintained at 37 °C in a saturated humidity atmosphere containing 95% air and 5% CO_2. Cells were seeded at density of $40 \times 10^3/cm^2$ in 6 wells culture dishes for the subsequent treatments. In a first set of experiments HEK cells were treated with H_2O_2 (Sigma–Aldrich, St Louis, MO, USA) 1–500 μM for 24 h to select the best dose of H_2O_2 to be used

Table 1
Autopsy case demographics.

Ref. N°	Groups	Age	Sex	Race	APOE	MMSE	PMI
1	AD	86	M	White	3/4	9	3.25
2	AD	87	F	White	3/3	0	2.67
3	AD	95	F	White	3/3	17	2.1
4	AD	90	M	White	3/4	12	3.25
5	AD	93	F	White	3/3	0	2.75
6	AD	83	M	White	NA	15	2.77
	Average	89				8.8	2.8
	SE	1.2				3.4	0.4
7	MCI	88	F	White	3/3	28	3
8	MCI	87	M	White	3/3	27	2,75
9	MCI	96	F	White	3/3	27	2,42
10	MCI	91	M	White	3/2	28	2,33
11	MCI	84	M	White	3/4	24	3,5
12	MCI	84	F	White	3/3	26	2,5
	Average	88.3				26.7	2.8
	SE	1.9				0.6	0.2
13	Control	85	F	White	3/3	30	2.12
14	Control	87	M	White	3/3	29	2.42
15	Control	92	M	White	3/3	30	3.75
16	Control	88	M	White	3/3	30	2.08
17	Control	84	F	White	3/3	30	2.42
	Average	87.2				29.8	2.5
	SE	1.3				0.2	0.3

in the other experiments. In a second set of experiments, aimed to demonstrate that the effects of H_2O_2 on GSK-3β were really due to the increase of intracellular oxidative stress, HEK cells were pre-treated with bilirubin (BR) 0.1–5 μM for 2 h, then the medium was discarded and cells were treated with 100 μM H_2O_2 μM for a further 24 h. Bilirubin (Sigma–Aldrich, St Louis, MO, USA) was dissolved in sodium hydroxide (0.1 M) at a concentration of 10 mM and further diluted in double-distilled water as previously described (Barone et al., 2009). Bilirubin solutions were freshly prepared before each experiment and protected from light. In a third set of experiments to test the effects produced by silencing *BVR-A*, HEK cells were seeded at density of $40 \times 10^3/cm^2$ in 6 wells culture dishes. After 24 h medium has been replaced with DMEM with 10% FBS, without antibiotics. Following, cells have been transfected with 10 pmol of a small-interfering RNA (siRNA) for BVR-A (Ambion, Life Technologies, LuBioScience GmbH, Lucerne, Switzerland, #4392420; sense sequence GACCUGGUCUAAA ACGAAAtt; antisense sequence UUUCGUUUUAGACCAGGUCct) using Lipofectamine® RNAiMAX reagent (Invitrogen, Life Technologies, LuBioScience GmbH, Lucerne, Switzerland, #13778-030) according to the manufacturer's protocol, and then treated with 100 μM H_2O_2 μM for 24 h. At the end of each treatment, cells were washed twice with PBS, collected and proteins were extracted as described below.

2.4. MTT assay

Cell viability was measured by the MTT reduction assay (Gerlier and Thomasset, 1986) as previously described (Perluigi et al., 2003). Briefly, HEK cells were plated in 96-well microplates at 1.5×10^4/well, eight replicas per condition. After overnight incubation, the medium was replaced with fresh medium containing H_2O_2 at concentrations ranging from 0 to 500 μM and further incubated for 24 h. Then, MTT was added at a final concentration of 1.25 mg/mL. After 2 h of incubation at 37 °C, medium was discarded and the reduced insoluble dye was extracted with 0.04 N HCl/isopropanol. Cell viability was evaluated by the absorbance ($A_{540–750}$) measured in a microplate reader (Labsystem Multiscan MS).

2.5. Samples preparation

Total protein extracts were prepared in RIPA buffer (pH 7.4) containing Tris-HCl (50 mM, pH 7.4), NaCl (150 mM), 1% NP-40, 0.25% sodium deoxycholate, EDTA (1 mM), 0.1% SDS, supplemented with protease inhibitors [phenylmethylsulfonyl fluoride (PMSF, 1 mM), sodium fluoride (NaF, 1 mM) and sodium orthovanadate (Na_3VO_4, 1 mM)]. Before clarification, brain tissues were homogenized by 20 passes with a Wheaton tissue homogenizer. Both brain tissues homogenates and collected cells were clarified by centrifugation for 1 h at 16,000 ×*g*, 4 °C. The supernatant was then extracted to determine the total protein concentration by the Bradford assay (Pierce, Rockford, IL).

2.6. Slot blot analysis

For the analysis of total Protein Carbonyls (PC) levels hippocampal total protein extract samples (5 μl), were derivatized with 5 μl of 10 mM 2,4-dinitrophenylhydrazine (DNPH) (OxyBlot™ Protein Oxidation Detection Kit, Merck-Millipore, Darmstadt, Germany) in the presence of 5 μl of 10% sodium dodecyl sulfate (SDS) for 20 min at room temperature (25 °C). The samples were then neutralized with 7.5 μl of neutralization solution (2 M Tris in 30% glycerol) and loaded onto nitrocellulose membrane as described below.

For total (i) protein-bound 4-hydroxy-2-nonenals (HNE) and (ii) 3-nitrotyrosine (3-NT) levels: hippocampal total protein extract samples (5 μl), 12% SDS (5 μl), and 5 μl modified Laemmli buffer containing 0.125 M Tris base, pH 6.8, 4% (*v*/v) SDS, and 20% (v/v) glycerol were incubated for 20 min at room temperature and then loaded onto nitrocellulose membrane as described below.

Proteins (250 ng) were loaded in each well on a nitrocellulose membrane under vacuum using a slot blot apparatus. The membrane was blocked in blocking buffer (3% bovine serum albumin) in PBS 0.01% (*w/v*) sodium azide and 0.2% (v/v) Tween 20 for 1 h and incubated with an anti-2,4-dinitrophenylhydrazone (DNP) adducts polyclonal antibody (1:100, EMD Millipore, Billerica, MA, USA, #MAB2223) or HNE polyclonal antibody (1:2000, Novus Biologicals, Abingdon, United Kingdom, #NB100-63093) or an anti 3-NT polyclonal antibody (1:1000, Santa Cruz, Santa Cruz, CA, USA, #sc-32757) in PBS containing 0.01% (w/v) sodium azide and 0.2% (v/v) Tween 20 for 90 min. The membrane was washed in PBS following primary antibody incubation three times at intervals of 5 min each. The membrane was incubated after washing with an anti-rabbit IgG alkaline phosphatase secondary antibody (1:5000, Sigma–Aldrich, St Louis, MO, USA) for 1 h. The membrane was washed three times in PBS for 5 min each and developed with Sigma fast tablets (5-bromo-4-chloro-3-indolyl phosphate/nitroblue tetrazolium substrate [BCIP/NBT substrate]). Blots were dried, acquired with Chemi-Doc MP (Bio-Rad, Hercules, CA, USA) and analyzed using Image Lab software (Bio-Rad, Hercules, CA, USA). No non-specific binding of primary or secondary antibodies to the membrane was observed.

2.7. Western blot

For western blots, 20 μg of proteins were resolved on Criterion TGX Stain-Free 4–15% 18-well gel (Bio-Rad Laboratories, #5678084) in a Criterion large format electrophoresis cell (Bio-Rad Laboratories, #1656001) in TGS Running Buffer (Bio-Rad Laboratories, #1610772). Immediately after electrophoresis, the gel was then placed on a Chemi/UV/Stain-Free tray and then placed into a ChemiDoc MP imaging System (Bio-Rad Laboratories, #17001402) and UV-activated based on the appropriate settings with Image Lab Software (Bio-Rad Laboratories) to collect total protein load image. Following electrophoresis and gel imaging, the proteins were transferred via the TransBlot Turbo semi-dry blotting apparatus (Bio-Rad Laboratories, #1704150) onto nitrocellulose membranes (Bio-Rad, Hercules, CA, USA, #162-0115) and membranes were blocked with 3% bovine serum albumin in 0.5% Tween-20/Tris-buffered saline (TTBS) and incubated overnight at 4 °C with the following antibodies: anti-BVR-A (1:5000, abcam, Cambridge, United Kingdom, #ab90491), anti-BVR-A (1:1000, Sigma-Aldrich, St Louis, MO, USA, #B8437), anti-Akt (1:1000, 1:1000,

Bio-Rad Laboratories, #vma00253k), anti-phospho(Ser473)-Akt (1:1000, Cell Signalling, Bioconcept, Allschwill, Switzerland, #193H12), anti-GSK-3β (1:500 Santa Cruz, Santa Cruz, CA, USA,#sc-9166), anti-phospho(Ser9)-GSK-3β (1:500 Santa Cruz, Santa Cruz, CA, USA,#sc-11,757), anti-phospho(Tyr216)- GSK-3β (1:500 Santa Cruz, Santa Cruz, CA, USA,#sc-135653), anti-Tau (1:1000, Santa Cruz, Santa Cruz, CA, USA, #sc-5587), anti 3-NT polyclonal antibody (1:1000, Santa Cruz, Santa Cruz, CA, USA, #sc-32757). The evaluation of Tau phosphorylation has been performed by using two different antibodies recognizing two different phosphorylated epitopes: anti-phospho (Ser404)-Tau (1:500, Santa Cruz, Santa Cruz, CA, USA, #sc-12952) which recognize Tau phosphorylated at Ser404 (target of GSK-3β), and anti-phospho(Ser416)-Tau (1:1000,Cell Signalling, Bioconcept, Allschwill, Switzerland, #15013), which recognize Tau phosphorylated at Ser416 (not listed among the residues target of GSK-3β activity). After 3 washes with TTBS the membranes were incubated for 60 min at room temperature with anti-rabbit/mouse/goat IgG secondary antibody conjugated with horseradish peroxidase (1:5000; Sigma–Aldrich, St Louis, MO, USA). Membranes were developed with Clarity ECL substrate (Bio-Rad Laboratories, #1705061) and then acquired with Chemi-Doc MP (Bio-Rad, Hercules, CA, USA) and analyzed using Image Lab software (Bio-Rad, Hercules, CA, USA) that permits the normalization of a specific protein signal with the β-actin signal in the same lane or total proteins load.

2.8. Immunoprecipitation

The immunoprecipitation procedure was performed as previously described (Cenini et al., 2008), with minor modifications. Immunoprecipitation experiment was performed using SureBeads™ Protein A Magnetic Beads (BioRad SureBeads™ Protein G #161-4023). Briefly,100 µl (100 µg) Surebeads were magnetized and washed with a solution of PBS/Tween20 0.1% *v*/v. as per manufacturer instructions, and then incubated for 30 min with 1 µg anti- GSK-3β polyclonal antibody (1:200, Santa Cruz, Santa Cruz, CA, USA,#sc-9166) at room temperature. After incubation, beads were washed 3 times with PBS/Tween20 0.1% v/v. After that, the beads/antibody complexes were recovered and incubated with 100 µg of protein extracts for 1 h at room temperature. Immunoprecipitated complexes were then pulled down and washed 3 times with PBS/Tween20 0.1% v/v. Immunoprecipitated GSK-3β was recovered by re-suspending the pellets in 2× Laemeli sample buffer and electrophoresing them on 12% gels, followed by western blot analysis. Total GSK-3β was used as a loading control as previously described (Barone et al., 2011a; Barone et al., 2011b; Lerner-Marmarosh et al., 2008; Salim et al., 2001).

2.9. Immunofluorescence

For immunocytofluorescent staining, cells were plated on coated glass coverslips for 24 h. Cells were washed three times with PBS and fixed in 4% paraformaldehyde for 30 min. After fixation, cells were washed twice with PBS and permeabilized for 30 min with permeabilization buffer composed by 0.2% Triton-X100 and PBS. Cells were blocked for 1 h with a solution containing 3% normal goat serum and 0.2% Triton X-100 in PBS and then were incubated overnight at 4 °C with following antibodies: anti-phospho(Ser404)-Tau (1:100, abcam, Cambridge, United Kingdom #ab92676), anti-phospho(Ser9)-GSK-3β (1:500 Santa Cruz, Santa Cruz, CA, USA,#sc-11757).Cells were washed with PBS and then incubated with Alexa Fluor -488 nm and -594 nm secondary antibodies (Invitrogen Corporation, Carlsbad, CA, USA) at 1:1000 for 1 h at room temperature. Cells were then washed again and incubated with DAPI solution. For each group of treatment staining was performed by omitting primary antibodies to establish nonspecific background signal. Cover slips were placed using a drop of Fluorimount (Sigma-Aldrich, St Louis, MO, USA).

All slides were imaged using Zeiss AXiocam (Carl Zeiss, Oberkochen, Germany). All immunolabeling acquisition intensities, field sizes, and microscopy settings were kept consistent across all images. Image montages for Figures were collated in Illustrator and Photoshop Cs6 (Adobe System, San Josè, CA, USA) software programs and were based upon cells that most closely approximated the group means.

2.10. Statistical analyses

All data were normalized against the respective control group and are expressed as mean ± SEM. Data were first tested for equal variance and normality (Shapiro–Wilk test) and the appropriate statistical tests were chosen. Changes in mice were evaluated separately at 6 and 12 months of age. For each variable, the 3xTg group was compared with the age-matched Non-Tg group. Student's and non-parametric *t*-test (Mann Whitney) were used to evaluate significant differences between Non-Tg and 3xTg mice. Human and cellular data were evaluated using one-way analysis of variance (ANOVA) with Bonferroni's Multiple Comparisons (and nonparametric ANOVA; Kruskal-Wallis). All statistical tests were two-tailed and the level of significance was set at 0.05. These analyses were performed using GraphPad Prism 7.0 software. Furthermore, a principle component analysis (PCA) was used to evaluate variance among variables involved in Tau phosphorylation both in mice and humans; results were generated by utilizing the built-in PCA function in XL-STAT.

3. Results

3.1. Early reduction of BVR-A protein levels is associated with reduced GSK-3β inhibition independently of Akt activation in the hippocampus of 3xTg-AD mice

We evaluated changes of BVR-A and oxidative stress levels along with alterations of (i) Akt protein and activatoring phosphorylation (Ser473) levels as well as (ii) changes of GSK-3β protein levels and inhibitory (Ser9) and activatoring (Tyr216) phosphorylations in the hippocampus of young (6 months) and old (12 months) 3xTg-AD mice compared to age-matched Non-Tg mice. Furthermore, downstream of GSK-3β we examined changes of Tau protein levels along with Tau phosphorylation at Ser404 [target of GSK-3β (Hanger and Noble, 2011; Leroy et al., 2010)] and Ser416 [non-target of GSK-3β (Hanger and Noble, 2011; Leroy et al., 2010)] residues.

We found that BVR-A protein levels were significantly reduced both at 6 months (−57%, $p < 0.05$, Fig. 1 A and B) and 12 months (−45%, $p < 0.05$, Fig. 1 A and 1 B) of age, in the hippocampus of 3xTg-AD mice with respect Non-Tg mice. In parallel, increased oxidative and nitrosative stress levels were observed both at 6 months (3-NT, +15%, $p < 0.05$, Fig. 1 C) and 12 months (PC, +10%, $p < 0.05$; 3-NT +47% $p < 0.001$; 4-HNE, +28%, $p < 0.001$, Fig. 1 D) of age in the hippocampus of 3xTg-AD with respect to Non-Tg mice.

The analyses of Akt protein revealed no significant changes at 6 months of age between 3xTg-AD and Non-Tg mice (Fig. 2 A and B), while a significant increase of Akt protein levels (+23%, $p < 0.05$) along with a significant decrease of Akt activation (Ser 473/Akt, −34%, $p < 0.05$) were observed in the hippocampus of 3xTg-AD with respect to Non-Tg mice at 12 months of age (Fig. 2 A and B).

Downstream of Akt, no changes of GSK-3β protein levels were observed either at 6 months or 12 months of age in 3xTg-AD with respect to Non-Tg mice (Fig. 2 A and 2C). GSK-3β inhibition (Ser9/GSK-3β) was significantly reduced both at 6 months (−26%, $p < 0.05$, Figs. 2 A and 2C) and at 12 months (−37%, $p < 0.05$, Figs. 2 A and C), without consistent changes of GSK-3β activation (Tyr216/GSK-3β) (Fig. 2 A and C). Taken together the GSK-3β inhibition/activation ratio (Ser9/Tyr216) was significantly decreased at 12 months (−51%, $p < 0.001$, Fig. 2 A and 2C) in 3xTg-AD with respect to Non-Tg mice.

With regard to Tau protein, we found that Tau Ser404

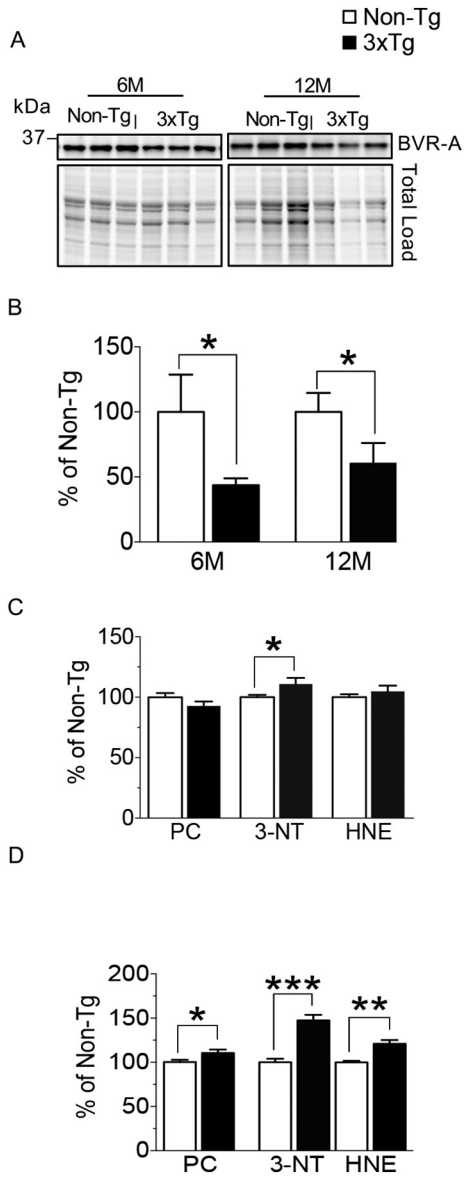

Fig. 1. Reduced BVR-A protein levels along with increased oxidative stress levels in the hippocampus of 3xTg-AD mice. Changes of BVR-A protein levels and levels of oxidative stress markers were evaluated in the hippocampus of 3xTg-AD mice and age-matched controls. (A) Representative western blot images and (B) densitometric evaluation of BVR-A protein levels evaluated in 3xTg-AD (n = 6/group) and age-matched Non-Tg mice (n = 6/group) both a 6 and 12 months of age. Protein levels were normalized per total protein load. Changes of protein carbonyls (PC), 4-hydroxyl-2-nonenals (HNE) and 3-nitrotyrosine (3-NT) levels in 3xTg-AD (n = 6/group) and age-matched Non-Tg mice (n = 6/group) both at **(C)** 6 and **(D)** 12 months of age. All densitometric values are given as percentage of Non-Tg mice set as 100%. Data are presented as means ± SEM, *p > 0.05, **p < 0.01, and ***p < 0.001 (Student's *t*-test; Mann-Whitney for HNE at 12 months of age).

phosphorylation was significantly increased both at 6 months (Ser404/Tau, +85%, p < 0.05, Fig. 2 A and D) and 12 months (+116%, p < 0.01, Fig. 2 A and D) of age, while Tau Ser416 phosphorylation was significantly increased only at 12 months (Ser416/Tau, +184%, p < 0.05, Fig. 2 A and D) in the hippocampus of 3xTg-AD with respect to Non-Tg mice.

Overall, these results suggest that reduced BVR-A protein levels are associated with reduced GSK-3β inhibition in the hippocampus of 3xTg-AD mice. This phenomenon is of particular interest at 6 months of age, when reduced GSK-3β inhibition occurs independently from changes of Akt activation and results in an early increased Tau Ser404 phosphorylation.

3.2. Reduced BVR-A protein levels are associated with reduced GSk-3β inhibition in post-mortem samples from human MCI inferior parietal lobule

To test whether the above-reported changes might be considered pathological features of AD, we analyzed inferior parietal lobule (IPL) post-mortem samples collected from amnestic mild cognitive impairment [MCI, a prodromal stage of AD (Petersen, 2003)], from AD and from age-matched control subjects. The choice of IPL was based on previous studies from the Butterfield group, showing that this brain region was characterized by increased oxidative stress along with increased Akt phosphorylation in both MCI and AD subjects although the inhibition of GSK-3β was evident only in AD subjects with respect to age-matched controls (Aluise et al., 2011; Sultana et al., 2010; Tramutola et al., 2015).

Reduced BVR-A protein levels in MCI with respect to age-matched controls were found [$F_{(2, 14)}$ = 3.88, p = 0.04, MCI vs Control: −30%, p < 0.01] (Fig. 3 A and B). No significant changes were observed for Akt protein levels and activation among the 3 groups of subjects (Fig. 3 A and C).

Downstream of Akt, we found a significant reduction of GSK-3β protein levels [$F_{(2, 14)}$ = 4.41, p = 0.03, AD vs Control: −33%, p < 0.05, Fig. 3 A and D] along with a significant increase of GSK-3β inhibition [Ser9/GSK-3β: $F_{(2, 14)}$ = 4.85, p = 0.02; AD vs Control: +126%, p < 0.05, Fig. 3 A and D] only in AD subjects with respect to age-matched controls. No significant changes were observed for GSK-3β activation (Try216/GSK-3β) in MCI and AD subjects with respect to controls. Taken together, a significant reduction of the GSK-3β inhibition/activation ratio in MCI subjects was observed, whereas a significant increase was found in AD subjects, with respect to age-matched controls [Kruskal-Wallis, p < 0.01; MCI vs Control:-76%, p < 0.05; AD vs Control: +161%, p < 0.05, Fig. 3 A and D].

Total Tau protein levels were significantly reduced only in AD subjects [$F_{(2, 14)}$ = 5.95, p = 0.01; AD vs Control: −66%, p < 0.01, Fig. 3 A and E] while Tau phosphorylation levels (Ser404/Tau) were significantly increased both in MCI and in AD with respect to age-matched controls [$F_{(2, 14)}$ = 7.83, p = 0.01; MCI vs Control: +91%, p < 0.05; AD vs Control: + 212%, p < 0.01, Fig. 3 A and E].

These results support the concept that reduced BVR-A levels are associated with an increased activation of GSK-3β, which favors Tau Ser404 phosphorylation also in humans. This effect seems prominent during the early stage of the pathology, i.e., MCI, since similar alterations in AD were not observed.

3.3. Loss of BVR-A limits the oxidative stress-induced Akt-mediated inhibition of GSK-3β in vitro

To clarify the molecular mechanisms responsible for the increase of GSK-3β activation during the early phase of AD, we used HEK cells to evaluate whether reduced BVR-A protein levels limit the oxidative stress-induced Akt-mediated inhibition of GSK-3β.

In a preliminary set of experiments, we tested the effects of increased oxidative stress levels on (i) cell viability, (ii) BVR-A protein levels, (iii) GSK-3β levels and activation, and (iv) Tau Ser404 phosphorylation levels by exposing HEK cells to increasing doses of H_2O_2 (1–500 μM) for 24 h. Among the tested doses we selected 100 μM, found to promote a significant increase of GSK-3β inhibition [$F_{(6, 28)}$ = 2.34, p = 0.04; Control vs H_2O_2: +31%, p < 0.05] along with reduced Tau phosphorylation [$F_{(6, 28)}$ = 3.13, p = 0.01; Control vs H_2O_2: +30%, p < 0.05] without affecting cell viability (Supplementary Fig. 1).

We confirmed the pro-oxidant effect mediated by 100 μM H_2O_2 by showing that H_2O_2-treated HEK cells were characterized by increased 3-NT levels [$F_{(5, 18)}$ = 16.63, p < .001; Control vs H_2O_2: +78%, p < 0001, Supplementary Fig. 2 A] and increased GSK-3β Ser9

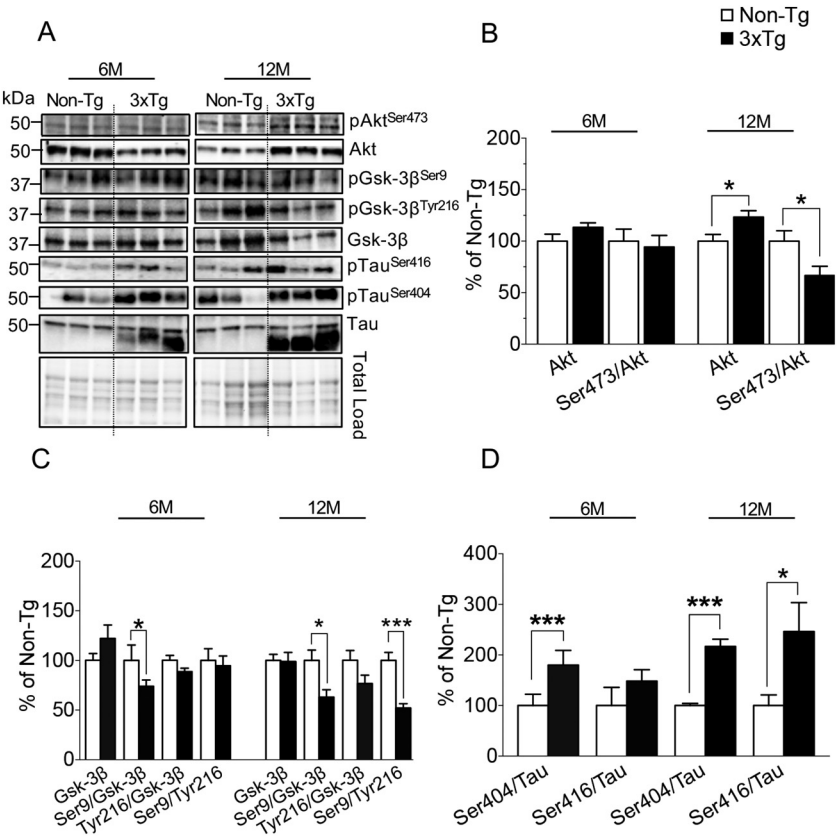

Fig. 2. Reduced inhibition of GSK-3β is associated with increased Tau Ser404 phosphorylation in the hippocampus of 3xTg-AD mice. Akt is one of the main kinases responsible for GSK-3β inhibition in response to increased oxidative stress levels and this process is favored by BVR-A, which works as scaffold protein. Changes of Akt protein levels and activation ($pAkt^{Ser473}$) along with with changes of GSK-3β protein levels, activation (pGSK-3βTyr216) and inhibition (pGSK-3βSer9) were evaluated in the hippocampus of 3xTg-AD mice and age-matched controls. Furthermore, changes of Tau phosphorylation at Ser404 (target of GSK-3β) and Ser416 (non-target of GSK-3β) residues were analyzed. (A) Representative western blot images and densitometric evaluation of (B) Akt protein levels and Ser473 phosphorylation; (C) GSK-3β protein levels, Ser9 and Tyr216 phosphorylation as well as Ser9/Tyr216 ratio; (D) Tau Ser404 and Ser416 phosphorylation evaluated in the hippocampus of 3xTg-AD (n = 6/group) and age-matched Non-Tg mice (n = 6/group) both at 6 and 12 months of age. Protein levels were normalized per total protein load. Akt-, GSK-3β-, and Tau-associated phosphorylations were normalized by taking into account the respective protein levels and are expressed as the ratio between the phosphorylated form and the total protein levels: Ser473/Akt, Ser9/GSK-3β, Tyr216/GSK-3β, Ser404/Tau and Ser416/Tau. All densitometric values are given as percentage of Non-Tg mice set as 100%. Data are presented as means ± SEM, *p < 0.05, **p < 0.01, and ***p < 0.001 (Student's t-test; Mann-Whitney for Ser473/Akt and Ser9/GSK-3β at 12 months of age).

phosphorylation [$F_{(5,\ 18)} = 2.72$, p = 0.05; Control vs H_2O_2: +34%, p < 0.05, Supplementary Figs. 2 B and 2 D] and that pre-treatment with increasing doses of bilirubin (BR, 0.1–5 μM for 2 h) – one of the most potent endogenous antioxidant (Barone et al., 2009; Mancuso et al., 2012) – abolished the effects of H_2O_2 (Supplementary Figs. 2 B, D and F).

Starting from these observations, we evaluated the effect of oxidative stress on GSK-3β and Tau protein in cells lacking BVR-A. This condition would mimic what we have observed both in mice and humans. The results show that while 100 μM H_2O_2 for 24 h promotes increased Akt Ser473 phosphorylation [$F_{(4,\ 15)} = 6.53$, p = 0.003; Control vs H_2O_2: +34%, p < 0.05 Fig. 4 A and C] along with increased GSK-3β inhibition [$F_{(4,\ 15)} = 20.16$, p < 0.001; Control vs H_2O_2 + 31%, p < 0.01, Fig. 4 A and D] and a significant reduction of Tau Ser404 phosphorylation [$F_{(4,\ 15)} = 4.28$, p = 0.016; Control vs H_2O_2: −36%, p < 0.01, Fig. 4 A and G] in control cells, these changes do not occur in cells lacking BVR-A. Indeed, in siRNA-treated cells, 100 μM H_2O_2 for 24 h led to a significant reduction of Akt Ser473 phosphorylation (−48%, p < 0.01, Fig. 4 A and C), a concomitant decreased GSK-3β inhibition (−64%, p < 0.001, Fig. 4 A and D) and a significant increased Tau Ser404 phosphorylation (+28%, p < 0.05 Fig. 4A and G), with respect to control cells treated with H_2O_2. No changes were found for total protein levels (Supplementary Fig. 4). Reduced GSK-3β inhibition and increased Tau Ser404 phosphorylation in cells lacking BVR-A and treated with H_2O_2 for 24 h were also confirmed by immunofluorescence analyses (Fig. 5).

Taken together, these results confirm our hypothesis that loss of BVR-A limits the Akt-mediated inhibition of GSK-3β in response to oxidative stress, thus resulting in increased Tau Ser404 phosphorylation.

3.4. Reduced BVR-A protein levels impair the interaction between Akt and GSK-3β

While the reduction of GSK-3β Ser9 phosphorylation observed in old 3xTg-AD mice (12 months) and in siRNA-treated cells exposed to H_2O_2 could be explained, at least in part, through the parallel reduction of Akt activation, it remained to understand whether BVR-A could play a role in the uncoupling of the Akt/GSK-3β axis observed in young 3xTg-AD mice and in MCI brain. Moreover, examination of the results collected in siRNA-treated cells and exposed to H_2O_2, suggested that an additional mechanism had to exist, other than the mere reduction of Akt activation. Indeed, the extent of the reduction of GSK-3β inhibition was much higher than the reduction of Akt activation in siRNA-treated cells exposed to H_2O_2 with respect to similarly exposed control cells.

For that reason, based on the well-known role for BVR-A to function as a scaffold protein (Gibbs et al., 2012; Kapitulnik and Maines, 2009; Miralem et al., 2016; Triani et al., 2018), we hypothesized that reduced BVR-A protein levels would impair the interaction between Akt and GSK-3β under oxidative stress conditions. Supporting this hypothesis, H_2O_2 treatment in HEK cells promotes the formation of the Akt/GSK-3β complex [$F_{(4,\ 15)} = 12.37$, p < 0.001; Control vs H_2O_2 + 50%, p < 0.01, Fig. 6 A and B], while this does not occur in cells lacking BVR-A (−85%, p < 0.001, Fig. 6 A and B). Immunofluorescence analyses supported the above results by showing that cells treated with H_2O_2 are characterized by increased levels of Akt Ser473 along with increased levels of GSK-3β Ser9 and that they co-localize. However, this does not occur in cells lacking BVR-A (Fig. 6 C—K). Moreover, a significant reduction of the Akt/GSK-3β complex levels in 3xTg-AD mice at 6 months of age with respect to Non-Tg (−58%, p < 0.05, Fig. 6 L and M) was found, while increased levels were observed in 12 months old 3xTg-AD mice (+50%, p < 0.05, Figs. 6 L and 6). Likewise, a reduction of the complex was observed in MCI samples with respect to age-matched controls [$F_{(2,\ 9)} = 3.6$, p = 0.04; MCI vs Control: −46%, p < 0.05] (Figures).

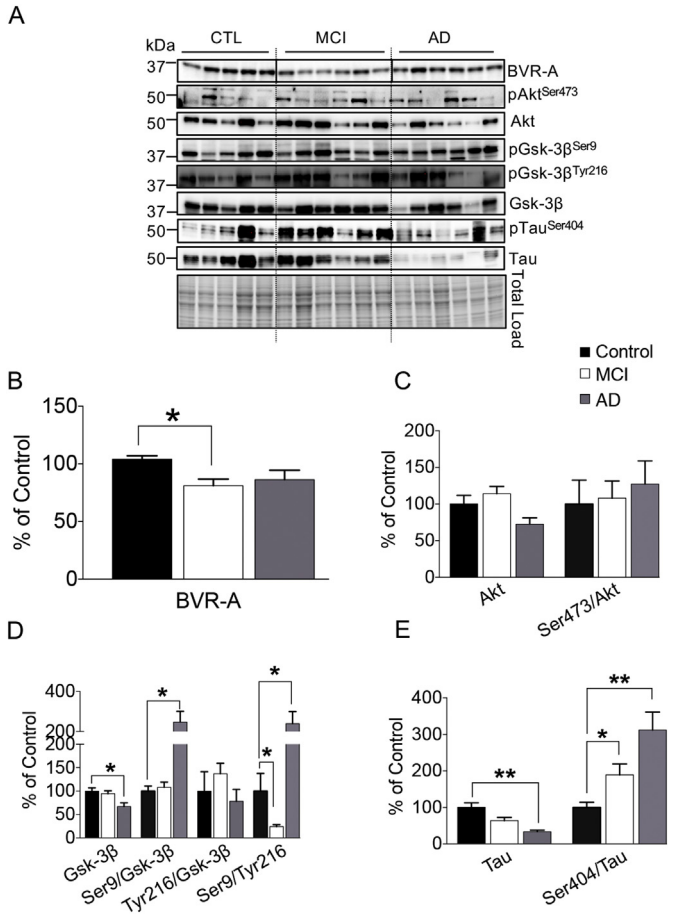

Fig. 3. Reduced BVR-A protein levels are associated with reduced GSK-3β inhibition and increased Tau Ser404 phosphorylation in human MCI subjects. Changes of BVR-A protein levels along with changes of (i) Akt protein levels and activation (pAkt^{Ser473}); (ii) GSK-3β protein levels, activation (pGSK-3βTyr216) and inhibition (pGSK-3βSer9) and (iii) Tau levels and phosphorylation at Ser404 residue (target of GSK-3β) were evaluated in the inferior parietal lobule (IPL) of Control, amnestic mild cognitive impairment (MCI) and Alzheimer's disease (AD) subjects. (A) Representative western blot images and densitometric evaluation of (B) BVR-A protein levels; (C) Akt protein levels and Ser473 phosphorylation; (D) GSK-3β protein levels, Ser9 and Tyr216 phosphorylation as well as Ser9/Tyr216 ratio; (E) Tau protein levels, Ser404 and Ser416 phosphorylation evaluated in IPL samples collected form Controls (n = 5) and age-matched MCI (n = 6) and AD (n = 6) subjects. Protein levels were normalized per total protein load. Akt-, GSK-3β-, and Tau-associated phosphorylations were normalized by taking into account the respective protein levels and are expressed as the ratio between the phosphorylated form and the total protein levels: Ser473/Akt, Ser9/GSK-3β, Tyr216/GSK-3β, Ser404/Tau. All densitometric values are given as percentage of Controls set as 100%. Data are presented as means ± SEM, *p < 0.05, **p < 0.01 (One-way ANOVA with Bonferroni *post-hoc* test; Kruskal-Wallis for GSK-3β Ser9/Tyr216 ratio).

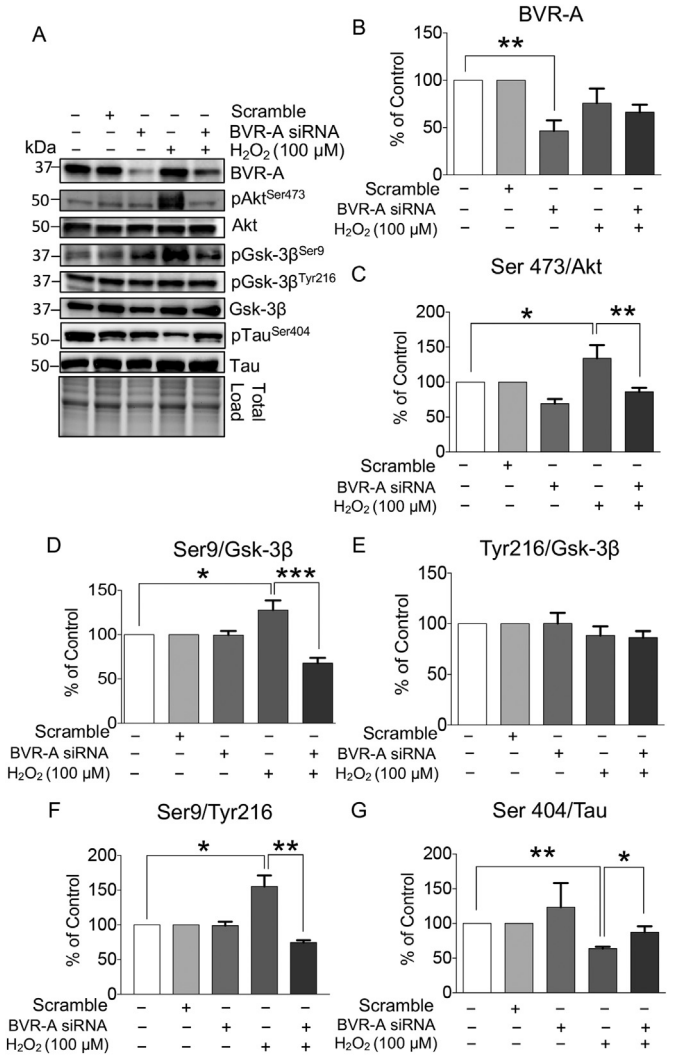

Fig. 4. Loss of BVR-A limits the oxidative stress-induced Akt-mediated inhibition of GSK-3β in HEK cells. The effect of increased oxidative stress levels on GSK-3β and Tau proteins in the absence of BVR-A was tested in HEK cells treated with H_2O_2. (A) Representative western blot images and densitometric evaluation of (B) BVR-A protein levels; (C) Akt Ser473 phosphorylation; (D) GSK-3β Ser9 phosphorylation (E) GSK-3β Tyr216 phosphorylation, (F) GSK-3β Ser9 /Tyr216 ratio; and (E) Tau Ser404 phosphorylation evaluated in HEK cells (n = 4 independent cultures/group) treated with H_2O_2 (100 μM, for 24 h) in the presence or not of BVR-A, whose silencing has been obtained through the use of a specific si-RNA. BVR-A protein levels were normalized per total protein load. Akt-, GSK-3β-, and Tau-associated phosphorylations were normalized by taking into account the respective protein levels and are expressed as the ratio between the phosphorylated form and the total protein levels: Ser473/Akt, Ser9/GSK-3β, Tyr216/GSK-3β, Ser404/Tau. All densitometric values are given as percentage of Controls cells set as 100%. Data are presented as means ± SEM, *p < 0.05, **p < 0.01, and ***p < 0.001 (ANOVA with Bonferroni *post-hoc* test).

These observations show that loss of BVR-A is associated with an impairment in the formation of the Akt/GSK-3β complex, which conceivably could explain why we observed a reduction of GSK-3β inhibition in spite of no changes of Akt activation.

3.5. Principal component analysis to examine the association among Tau phosphorylation, oxidative stress and GSK-3β

PCA calculates the components that explain the largest amount of variance whereas a biplot displays how much the variables contribute to variance for the two most predominant PCA-identified components (Fig. 7).

PCA in mice, show that that component 1 (F1) accounts for 49,90% of the variance and it is dominated by GSK-3β activation (Ser9/GSK-3β, GSK-3β Ser9/Tyr216 ratio), Tau phosphorylation (Ser404/Tau) and oxidative stress (3-NT), while component 2 (F2) accounts for 21,67% of the variance and it is dominated by BVR-A and Akt activation (Fig. 7 A-C).

Similarly, PCA in human samples show that component 1 accounts for 47,49% of the variance and it is dominated by GSK-3β activation (Ser9/GSK-3β, GSK-3β Ser9/Tyr216 ratio), while component 2 accounts for 20.73% of the variance and it is dominated by BVR-A.

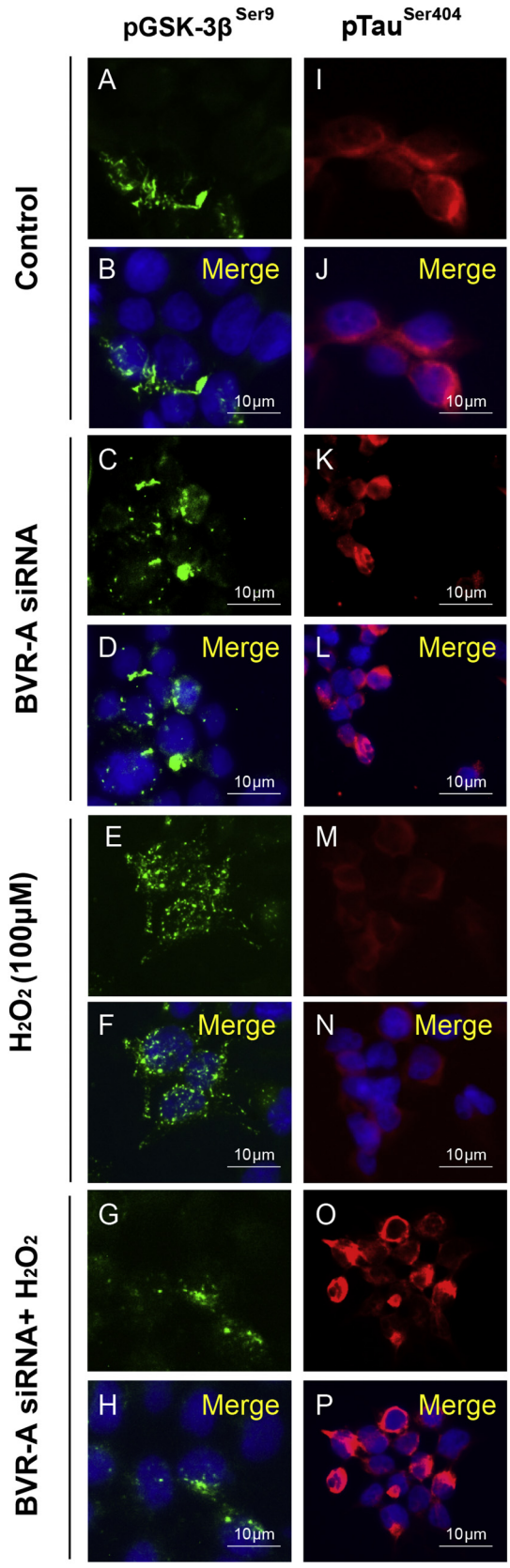

Fig. 5. Reduced GSK-3β inhibition along with increased Tau Ser404 phosphorylation in response to increased oxidative stress in HEK cells. Representative immunofluorescence images (40× objective) from fixed (4% PAF) HEK cells stained with anti-pGSK-3β^{Ser9} (green) and pTau^{Ser404} (red) in the following conditions: control (A-B and I-J); BVR-A siRNA (C-D and K-L); H_2O_2 (100 μM, for 24 h) (*E*-F and M-N); and BVR-A siRNA +100 μM H_2O_2 (G-H and O—P). DAPI (blue) was used to identify cell nuclei. Scale bar represents 10 μm. (For interpretation of the references to colour in this figure legend, the reader is referred to the web version of this article.)

4. Discussion

In this paper we show for the first time that a reduction of BVR-A protein levels would impair the oxidative stress-induced Akt-mediated inhibition of GSK-3β during the development of AD pathology. Indeed, activation of the GSK-3β pathway has been shown to affect neuronal survival and synaptic plasticity by promoting Tau phosphorylation (Anderton et al., 2001; Mandelkow et al., 1992; Pei et al., 1999). In the brain from AD subjects and mouse model, altered localization of GSK-3β is associated with NFTs formation(Baum et al., 1996; Ishizawa et al., 2003; Lucas et al., 2001; Pei et al., 1997). During the early stage of AD development, GSK-3β accumulates with Tau in the cytoplasm of pre-tangle neurons (Pei et al., 1997), whereas in mature NFTs, the co-localization with GSK-3β is reduced(Baum et al., 1996; Harr et al., 1996; Shiurba et al., 1996). In addition, overexpression of active GSK-3β results in an AD-like phenotype(Brownlees et al., 1997), that can be reversed by reducing GSK-3β levels(Engel et al., 2006; Farr et al., 2014; Lucas et al., 2001). These lines of evidence, therefore, indicate that the activation of GSK-3β is a key, early event promoting Tau phosphorylation in AD(Rockenstein et al., 2007).

Our findings strengthen the above-cited data and propose a novel molecular mechanism, which may be responsible for the aberrant activation of GSK-3β and the consequent increase of Tau phosphorylation in early stage AD. In particular, we show that loss of BVR-A is associated with the uncoupling of the Akt/GSK-3β proteins in response to oxidative stress, and therefore loss of BVR-A might contribute to the pathological activation of GSK-3β. This aspect is significant because the Akt/GSK-3β complex is a target of multiple signalling cascades activated in response to different pro-survival stimuli (Hermida et al., 2017; Manning and Toker, 2017) and found to be altered in AD (Zhang et al., 2018). In parallel, BVR-A was demonstrated to participate in a number of intracellular processes regulated by Akt, including energy metabolism, gene expression, cell proliferation, and survival (Barone et al., 2014; Kapitulnik and Maines, 2009), thus consistent with the notion of a mutual interaction.

Previous studies from our group showed that reduced BVR-A activation triggers the development of brain insulin resistance in 3xTg-AD mice (Barone et al., 2016). We demonstrated that oxidative stress leads to reduced BVR-A Tyr phosphorylation, thus making BVR-A less active. In turn, reduced BVR-A activity is responsible for IRS1 hyper-activation, which is not associated downstream with a parallel activation of Akt (Barone et al., 2016; Barone et al., 2018). Of note, intranasal insulin administration prevents BVR-A impairment and the alterations of IRS1/Akt axis (Barone et al., 2018).

The above-cited observations together with current findings support the idea that BVR-A is at the cross-roads between: (1) the activation of the insulin signalling cascade and (2) the cell stress response in AD, both having Akt as a molecular target (Manning and Toker, 2017). In this scenario, we provide novel evidence about the loss of Akt-mediated inhibition of GSK-3β in the hippocampus of 3xTg-AD mice and in MCI subjects, which agree with the proposed role for GSK-3β in contributing significantly to Tau phosphorylation in AD.

The increased activation of GSK-3β observed in the hippocampus of 3xTg-AD mice both at 6 and 12 months of age, seems to be due to a reduction of Ser9 phosphorylation rather than an increase of Tyr216 phosphorylation (Fig. 2), thus strengthening the hypothesis about the

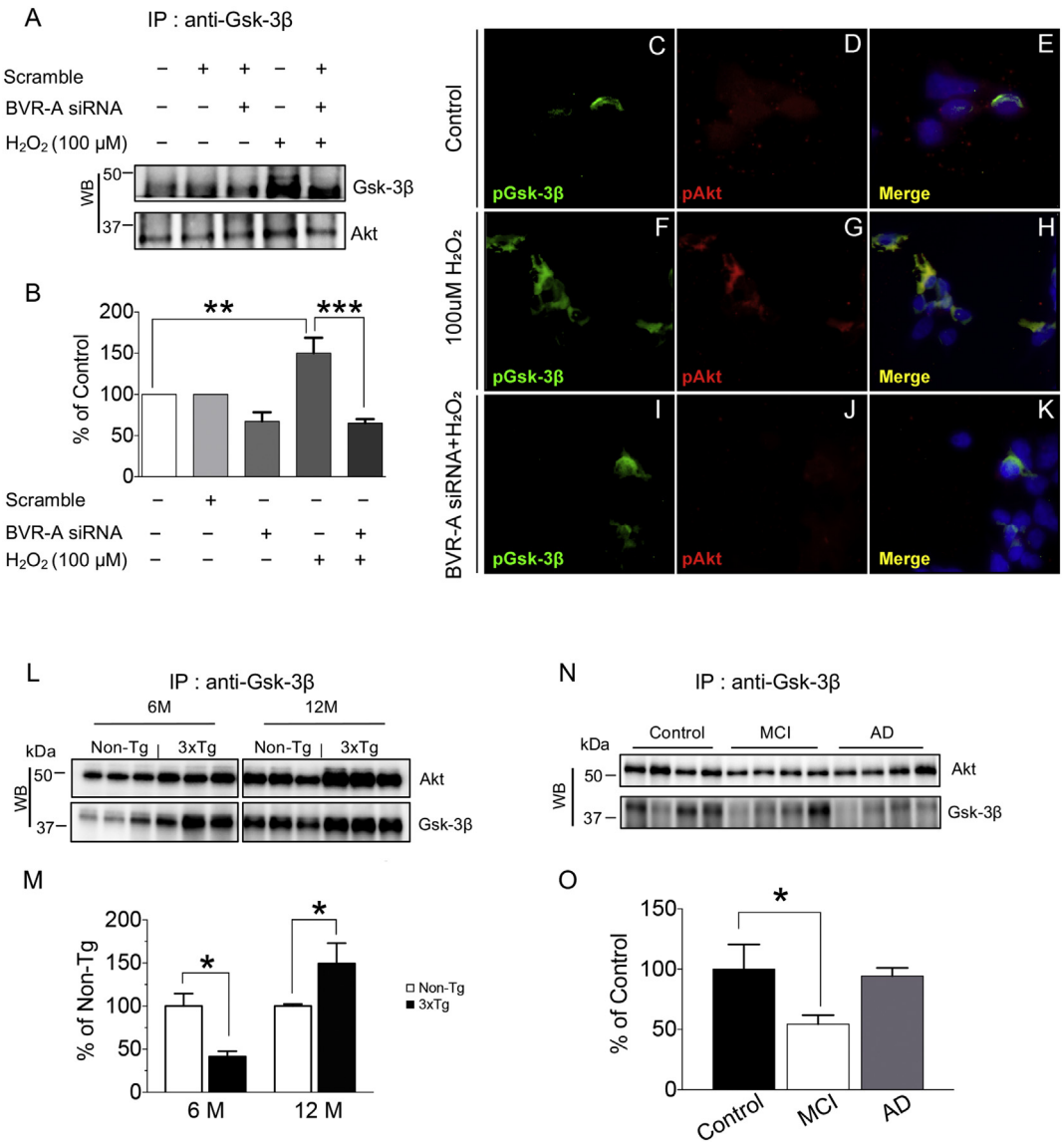

Fig. 6. Loss of BVR-A impairs the physical interaction between Akt and GSK-3β in response to oxidative stress. Based on the role for BVR-A to work as a scaffold protein, we tested whether reduced BVR-A protein levels would impair the physical interaction between Akt and GSK-3β proteins under oxidative stress conditions. **(A)** Representative western blot images and (B) densitometric evaluation of the Akt/GSK-3β complex isolated from HEK cells (n = 4 independent cultures/group) treated with H_2O_2 (100 μM, for 24 h) in the presence or not of BVR-A, whose silencing has been obtained through the use of a specific si-RNA; (C–K) Representative immunofluorescence images (40× objective) from fixed (4% PAF) HEK cells stained with anti-pGSK-3β^{Ser9} (green) and pAkt^{Ser473} (red) in the following conditions: **(C-E)** control; (F–H) H_2O_2 (100 μM, for 24 h); and (I–K) BVR-A siRNA + 100 μM H_2O_2. DAPI (blue) was used to identify cell nuclei. Scale bar represents 10 μm. (L-O) Representative western blot images and densitometric evaluation of the Akt/GSK-3β complex isolated from (L-M) hippocampal samples collected from 3xTg-AD and Non-Tg mice at 6 (n = 6/group) and 12 (n = 6/group) months of age; and (N–O) IPL samples collected from Control (n = 4), MCI(n = 4) and AD (n = 4) subjects. In (A-B, L-M and N–O) Akt levels bound GSK-3β were normalized by using total GSK-3β as loading control. All densitometric values are given as percentage of (B) Controls cells, (M) Non-Tg mice and (O) Control subjects set as 100%. Data are presented as means ± SEM, *p < 0.05, **p < 0.01, and ***p < 0.001 (Student's t-test or ANOVA with Bonferroni *post-hoc* test). (For interpretation of the references to colour in this figure legend, the reader is referred to the web version of this article.)

loss of Akt-mediated inhibition (Manning and Toker, 2017). This latter aspect is further supported by the increase of Tau Ser404 phosphorylation, which is significantly elevated at 6 months and persists in old 3xTg-AD mice at 12 months of age (Fig. 2). Indeed, GSK-3β is able to phosphorylate Tau at multiple sites (Godemann et al., 1999; Liu et al., 2004; Llorens-Martin et al., 2014) although the most prominent phosphorylation sites are Ser396 and Ser404 (PHF-1 epitope)(Agarwal-Mawal et al., 2003; Godemann et al., 1999; Lovestone et al., 1996; Sun et al., 2002). Phosphorylation at Ser396 and Ser404 seems to precede phosphorylation at the other sites on Tau (Godemann et al., 1999). Although GSK-3β preferentially phosphorylates many of its substrates after they have been pre-phosphorylated by other kinases, the stretch of amino acids in Tau that includes the residues Ser396, Ser400, and Ser404, can be directly phosphorylated by GSK-3β without the prior activity of other kinases(Hanger and Noble, 2011; Leroy et al., 2010). However, phosphorylation at Ser404 is critical to this process, and substitution of this residue by alanine ablates phosphorylation of both Ser396 and Ser400. It appears, therefore, that the primary phosphorylation of Ser404 by GSK-3β can itself serve as a primed residue for the subsequent sequential phosphorylation of Tau at Ser400 and Ser396 by GSK-3β (Hanger and Noble, 2011; Leroy et al., 2010).

Data collected in MCI (Fig. 3), showing reduced GSK-3β inhibition without significant changes of Akt activation (Fig. 3) despite increased oxidative stress (Aluise et al., 2011), reinforce the hypothesis that

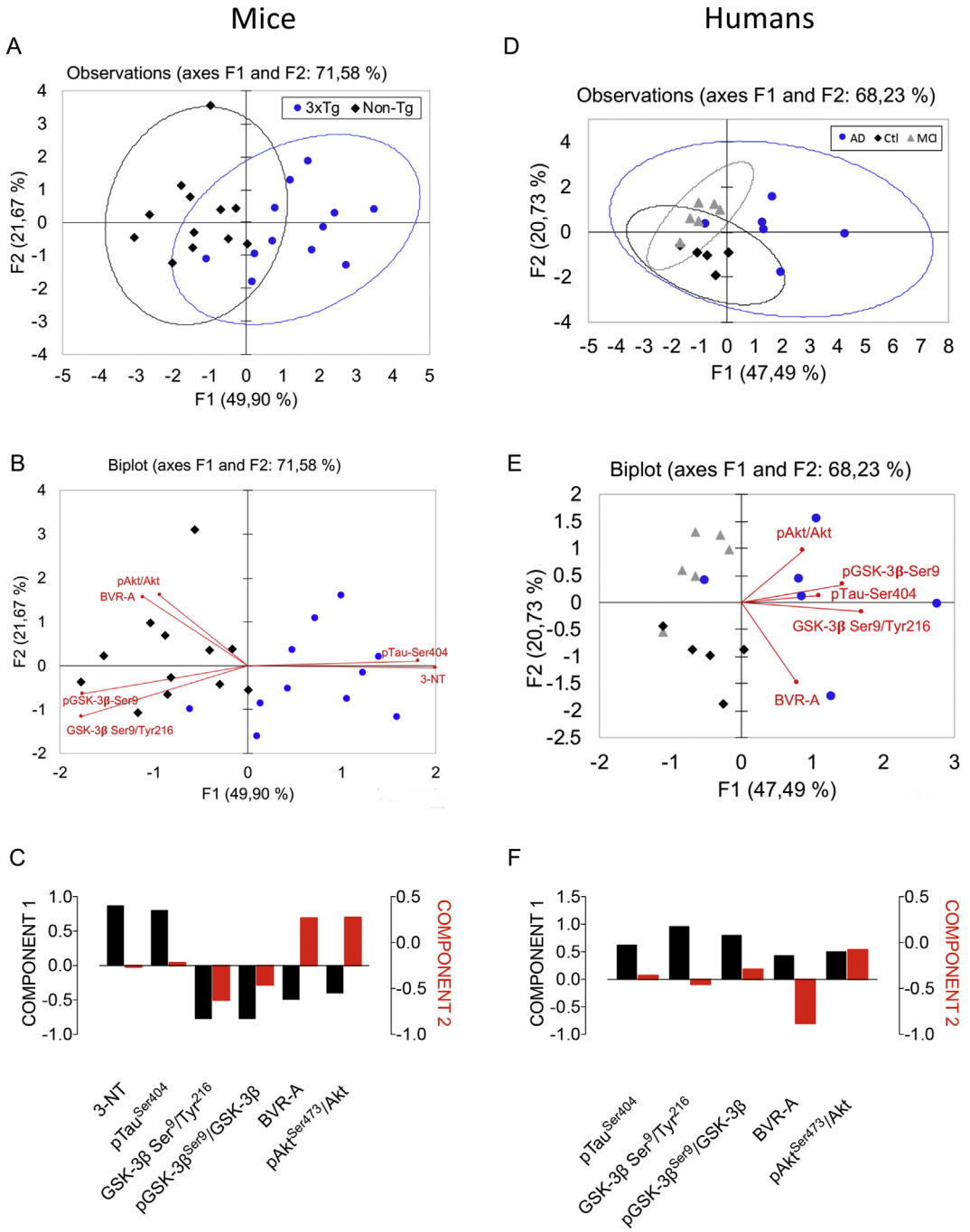

Fig. 7. Principal component analysis results collected in mice and human samples. Principal component analysis (PCA) was performed on the results collected in mice (A-C) and human samples (D-F) to determine variance contribution of the key components associated with Tau phosphorylation. Through this analysis we aimed to strength our hypothesis that changes of GSK-3β activation and Tau phosphorylation in response to oxidative stress were associated with changes of BVR-A. Variables mostly representative of the molecular mechanisms underlying Tau phosphorylation, were included in the analyses: 1. BVR-A protein levels (since BVR-A works as scaffold protein favoring the interaction between Akt and GSK-3β); 2. Akt activation (Ser473/Akt, since active Akt is responsible for GSK-3β inhibition); 3. GSK-3β Ser9 phosphorylation (Ser9/GSK-3β, since Ser9 is target of Akt activity and is responsible for GSK-3β inhibition); 4. GSK-3β Ser9/Tyr216 ratio (as additional measure of GSK-3β activation state); 5. Tau Ser404 phosphorylation (Ser404/Tau, since Ser404 is target of GSK-3β activity); and 6. 3-NT levels (as marker of oxidative stress elevated both at 6 and 12 months of age in 3xTg-AD mice). Same variables were used to perform PCA in human samples except 3-NT, since oxidative stress markers were not evaluated in the current study. In (A,B) and (D,E) scores plots and biplots graphs for mice and humans, respectively. Scores plot displays the observations coordinates on the PCA dimensions, while the biplot graphs represent the observations and variables simultaneously in the new space. Component 1 (F1) accounted for 49,9% and component 2 (F2) accounted for 21,67% of the variance in mice (A, B). F1 accounted for 47,49% and F2 accounted for 20,73% of the variance in humans (D,E). Contribution of each variable to component 1 (black bars) and component 2 (red bars) expressed as factor loadings is shown in (C) for mice samples and in (F) for human samples. These values represent the extent to which each variable contributed to building the corresponding PCA axis. Both in mice and humans F1 was dominated by GSK-3β activation and Tau phosphorylation, while F2 by BVR-A, thus suggesting that these 3 proteins influence each other. (For interpretation of the references to colour in this figure legend, the reader is referred to the web version of this article.)

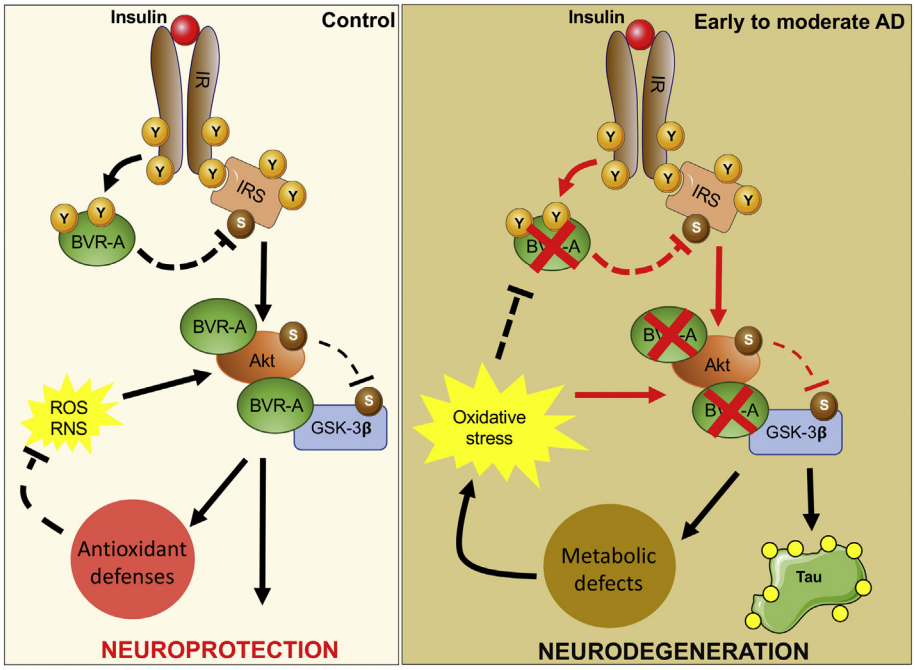

Fig. 8. Schematic representation of the proposed mechanism through which loss of BVR-A impairs the Akt-mediated inhibition of GSK-3β in Alzheimer's disease. *Left panel:* binding of insulin to insulin receptor (IR) promotes IR auto-phosphorylation on Tyr (Y) residues, which is responsible for the activation of IR kinase activity. Then, IR phosphorylates both biliverdin reductase-A (BVR-A) and the insulin receptor substrate (IRS) on specific Y residues responsible for their respective activation. Activated BVR-A regulates IRS, by phosphorylating IRS on inhibitory serine (S) residues, thus avoiding IRS abnormal activation. In turn, activated IRS recruits downstream proteins [e.g. phosphatidil-insoitol 3 kinase (PI3K)], responsible for Akt phosphorylation and activation. Once activated, Akt mediates the phosphorylation of GSK-3β on Ser9 promoting GSK-3β inhibition. In parallel, the Akt-mediated GSK-3β inhibition occur in response to an eventual increase of pro-oxidant species [e.g., reactive oxygen species (ROS), reactive nitrogen species (RNS)], with the aim to promote the cellular antioxidant defenses to counteract the rise of oxidative stress. Both the correct activation of Akt and the Akt-mediated GSK-3β inhibition are favored by BVR-A, which functions as a scaffold protein. All together these molecular events characterize the physiological activation of the insulin signalling cascade and those of the cell stress response, which confer neuroprotection to the brain. *Right panel:* during the progression of Alzheimer's disease (AD) pathology reduced BVR-A levels represent a harmful event, which impairs insulin signalling: (a) upstream, at the level of IRS, at which loss of BVR-A is responsible for IRS hyper-activation; and (b) downstream of IRS, where loss of BVR-A causes either the reduced activation of Akt or the impairment of the Akt/GSK-3β complex, which results in reduced GSK-3β inhibition. All together these molecular alterations would favor the anomalous activation of insulin signalling causing metabolic defects finally responsible for increased oxidative stress levels. As in a vicious cycle, increased oxidative stress further impairs BVR-A contributing to maintain hyper-active IRS. In parallel, loss of BVR-A precludes the activation of Akt (in response to either hyper-active IRS or oxidative stress), and the consequent inhibition of GSK-3β, thus resulting in hyper-active GSK-3β. This latter event leads to Tau hyper-phosphorylation responsible for neurodegeneration in AD. *Black arrows: activation; black dotted lines: inhibition; red arrows and red dotted lines: disrupted in AD.* (For interpretation of the references to colour in this figure legend, the reader is referred to the web version of this article.)

increased GSK-3β activation may represent an early event during the progression of AD pathology (Nicolia et al., 2017; Steen et al., 2005).

Noteworthy, under oxidative stress conditions loss of BVR-A would seem to impair the Akt-mediated inhibition of GSK-3β via two mechanisms: (1) by precluding the activation of Akt; and (2) by avoiding the physical interaction between Akt and GSK-3β. The first mechanism is consistent with previous data from Maines' group (Miralem et al., 2016) and helps to explain the results collected in old 3xTg-AD mice in which reduced Akt activation is associated with reduced GSK-3β inhibition. The second mechanism is completely novel and conceivably can explain the uncoupling of Akt and GSK-3β in young 3xTg-AD mice (Fig. 2) as well as in MCI (Fig. 3).

Our data demonstrate that oxidative stress promotes the phosphorylation of Akt and the inhibition of GSK-3β in control cells but not in cells lacking BVR-A (Fig. 4). Increased Akt phosphorylation following H_2O_2 is a physiological mechanism through which cells counteract toxic effects of oxidative stress (Chong et al., 2005), also by inhibiting GSK-3β (Chong et al., 2005). Accordingly, treatment with a GSK-3β inhibitor protected against H_2O_2-induced mitochondrial dysfunction and apoptotic DNA fragmentation in HEK cells (Shin et al., 2004). Conversely, the effect of H_2O_2 becomes detrimental if it is associated with a reduction of BVR-A (Fig. 4). Indeed, loss of BVR-A blocks H_2O_2-induced activation of Akt and precludes the association between Akt and GSK-3β, thus impeding the physiological inhibition of GSK-3β. This results in a dysregulated phosphorylation of Tau Ser404 (Fig. 4), which would become more prone to aggregate as NFTs (Wang and Mandelkow, 2016).

The proposed mechanism is thought to occur in the early phases of AD pathology, in both humans (MCI, Fig. 3) and mice (Fig. 2 and Fig. 1), where elevated oxidative stress parallel (i) reduced BVR-A levels and (ii) reduced GSK-3β inhibition. In contrast, increased Akt phosphorylation along with increased GSK-3β inhibition without changes in their interaction in late stage AD (Fig. 6) agree with others and our previous studies (Griffin et al., 2005; Pei et al., 2003; Tramutola et al., 2015; Yarchoan et al., 2014). Surprisingly, we observed increased Akt/GSK-3β complex levels in the brain of old 3xTg-AD mice (Fig. 6). Despite of that, the interaction appears not successful since reduced Akt activation along with reduced GSK-3β inhibition were observed (Fig. 2), in agreement with our hypothesis.

PCA further highlights that Tau phosphorylation is closely associated with changes of oxidative stress, GSK-3β and BVR-A (Fig. 7). Indeed, Tau phosphorylation and GSK-3β activation contribute substantially to the variance both in mice and human samples, thus strengthening the role of GSK-3β in Tau phosphorylation in AD. Furthermore, PCA in mice samples show that Tau phosphorylation and oxidative stress levels closely align in PCA component 1, suggesting that increased oxidative stress levels influence Tau phosphorylation. In addition, in both PCA analyses BVR-A is the predominant variable associated with component 2, thus underlying the role played by this protein in the molecular mechanisms responsible for Tau phosphorylation. These results are in line with those provided by Huber et al. proposing GSK-3β as primary contributor to Tau phosphorylation and the consequent cognitive decline observed in 3xTg-AD mice (Huber et al., 2018)

In particular, the meta-analysis performed in the above-cited study suggests that Tau phosphorylation has the strongest correlation to cognitive decline observed in 3xTg-AD mice, than any of the other assessed clinical outcomes measures, including Aβ (Huber et al., 2018). In this frame, we acknowledge that our study was designed to evaluate the role of BVR-A in the Akt-mediated inhibition of GSK-3β inhibition in response to oxidative stress in AD and therefore we looked at Tau protein (as target of GSK-3β activity along the progression of AD) but not at Aβ levels. Notwithstanding, our previous findings in 3xTg-AD mice show that improvement of BVR-A activation following intranasal

insulin administration is associated with reduced Tau phosphorylation and improved cognitive functions in 3xTg-AD mice both at 6 and 12 months of age (Barone et al., 2018), conversely, a reduction of Aβ56 oligomers is evident only later, at 12 months of age (Di Domenico et al., 2013). Although we cannot exclude the contribution of other Aβ forms, which in any case were shown to increase early in 3xTg-AD mice (Belfiore et al., 2018), our results are in line with the proposed role for Tau phosphorylation as a major contributor to cognitive decline in 3xTg-AD mice.

We propose a regulatory network in which BVR-A dysfunction may alter the physiological response to oxidative stress and insulin, thus resulting in increased Tau phosphorylation. Indeed, we found that the reduction of brain resident BVR-A is evident at 3 months of age, even before significant increased oxidative stress (Barone et al., 2016), in 3xTg-AD mice. Conceivably, reduced BVR-A levels could lead to alterations of the insulin signalling cascade, which would trigger metabolic defects favoring increased oxidative stress (de la Monte, 2009; de la Monte and Tong, 2014; Neumann et al., 2008). In turn, oxidative stress would impair BVR-A kinase activity, favoring the pathological activation of IRS1 (Barone et al., 2016). At this point, despite increased oxidative stress and IRS1 activation, reduced BVR-A protein levels would impede the correct activation of Akt and the following inhibition of GSK-3β. As result, an increased Tau phosphorylation occurs (Fig. 8).

The proposed paradigm is consistent with previous studies showing an association among oxidative stress, brain insulin resistance and increased Tau phosphorylation in AD (Butterfield et al., 2014; Chatterjee and Mudher, 2018; Cheng et al., 2005; Schubert et al., 2003; Schubert et al., 2004).

5. Conclusions

Overall, our results shed new light on the early mechanisms contributing to the development of AD pathology. In particular, we provide support for a novel link among increased oxidative stress, alterations of the insulin-signalling cascade, and the development of Tau pathology, having BVR-A as the central player. This mechanism is of interest because elucidating the early mechanisms promoting the aberrant activation of GSK-3β is critical for the identification of new therapeutic strategies to slow/prevent AD neuropathology. We are aware of the vast complexity of AD pathology and that it likely will require a combination treatment to achieve significant clinical effects. However, we also believe that the role of GSK-3β needs to be revisited in light of our and other findings showing GSK-3β hyper-activation in early but not late AD. Therefore, any treatment aimed to restore GSK-3β activity should be administered when the protein is hyper-activated. This event is likely to occur early in MCI or moderate AD, and future clinical studies in AD should take this aspect into considerations.

Conflict of interest

The authors declare no conflict of interests exist.

Acknowledgements

Authors acknowledge the contribution of Dr. Danilo Alunni-Fegatelli for his kind help in performing PCA analysis. This work was supported by funding from Banca d'Italia n° 12868/17 to EB; by founding from the Ministry of Education, Universities and Research (MIUR) under the SIR program n° RBSI144MT to FDD; by funding from Fondi Ateneo grant funded by Sapienza University n° C26H15JT9X to MP. We thank the Sanders-Brown Center of Aging of the University of Kentucky for providing us with well-characterized IPL specimens from MCI and AD brains and their age-matched controls.

Appendix A. Supplementary data

Supplementary data to this article can be found online at https://doi.org/10.1016/j.nbd.2019.02.003.

References

Agarwal-Mawal, A., Qureshi, H.Y., Cafferty, P.W., Yuan, Z., Han, D., Lin, R., Paudel, H.K., 2003. 14-3-3 connects glycogen synthase kinase-3 beta to tau within a brain microtubule-associated tau phosphorylation complex. J. Biol. Chem. 278, 12722–12728.

Aluise, C.D., Robinson, R.A., Beckett, T.L., Murphy, M.P., Cai, J., Pierce, W.M., Markesbery, W.R., Butterfield, D.A., 2010. Preclinical Alzheimer disease: brain oxidative stress, Abeta peptide and proteomics. Neurobiol. Dis. 39, 221–228.

Aluise, C.D., Robinson, R.A., Cai, J., Pierce, W.M., Markesbery, W.R., Butterfield, D.A., 2011. Redox proteomics analysis of brains from subjects with amnestic mild cognitive impairment compared to brains from subjects with preclinical Alzheimer's disease: insights into memory loss in MCI. J. Alzheimers Dis. 23, 257–269.

Anderton, B.H., Betts, J., Blackstock, W.P., Brion, J.P., Chapman, S., Connell, J., Dayanandan, R., Gallo, J.M., Gibb, G., Hanger, D.P., Hutton, M., Kardalinou, E., Leroy, K., Lovestone, S., Mack, T., Reynolds, C.H., Van Slegtenhorst, M., 2001. Sites of phosphorylation in tau and factors affecting their regulation. Biochem. Soc. Symp. 73–80.

Barone, E., Trombino, S., Cassano, R., Sgambato, A., De Paola, B., Di Stasio, E., Picci, N., Preziosi, P., Mancuso, C., 2009. Characterization of the S-denitrosylating activity of bilirubin. J. Cell. Mol. Med. 13, 2365–2375.

Barone, E., Di Domenico, F., Cenini, G., Sultana, R., Cini, C., Preziosi, P., Perluigi, M., Mancuso, C., Butterfield, D.A., 2011a. Biliverdin reductase-A protein levels and activity in the brains of subjects with Alzheimer disease and mild cognitive impairment. Biochim. Biophys. Acta 1812, 480–487.

Barone, E., Di Domenico, F., Cenini, G., Sultana, R., Coccia, R., Preziosi, P., Perluigi, M., Mancuso, C., Butterfield, D.A., 2011b. Oxidative and nitrosative modifications of biliverdin reductase-A in the brain of subjects with Alzheimer's disease and amnestic mild cognitive impairment. J. Alzheimers Dis. 25, 623–633.

Barone, E., Mancuso, C., Di Domenico, F., Sultana, R., Murphy, M.P., Head, E., Butterfield, D.A., 2012. Biliverdin reductase-A: a novel drug target for atorvastatin in a dog pre-clinical model of Alzheimer disease. J. Neurochem. 120, 135–146.

Barone, E., Di Domenico, F., Mancuso, C., Butterfield, D.A., 2014. The Janus face of the heme oxygenase/biliverdin reductase system in Alzheimer disease: it's time for reconciliation. Neurobiol. Dis. 62, 144–159.

Barone, E., Di Domenico, F., Cassano, T., Arena, A., Tramutola, A., Lavecchia, M.A., Coccia, R., Butterfield, D.A., Perluigi, M., 2016. Impairment of biliverdin reductase-A promotes brain insulin resistance in Alzheimer disease: a new paradigm. Free Radic. Biol. Med. 91, 127–142.

Barone, E., Tramutola, A., Triani, F., Calcagnini, S., Di Domenico, F., Ripoli, C., Gaetani, S., Grassi, C., Butterfield, D.A., Cassano, T., Perluigi, M., 2018. Biliverdin Reductase-A mediates the beneficial effects of intranasal insulin in Alzheimer Disease. Mol. Neurobiol. https://doi.org/10.1007/s12035-018-1231-5.

Baum, L., Hansen, L., Masliah, E., Saitoh, T., 1996. Glycogen synthase kinase 3 alteration in Alzheimer disease is related to neurofibrillary tangle formation. Mol. Chem. Neuropathol. 29, 253–261.

Belfiore, R., Rodin, A., Ferreira, E., Velazquez, R., Branca, C., Caccamo, A., Oddo, S., 2018. Temporal and regional progression of Alzheimer's disease-like pathology in 3xTg-AD mice. Aging Cell e12873.

Bomfim, T.R., Forny-Germano, L., Sathler, L.B., Brito-Moreira, J., Houzel, J.C., Decker, H., Silverman, M.A., Kazi, H., Melo, H.M., McClean, P.L., Holscher, C., Arnold, S.E., Talbot, K., Klein, W.L., Munoz, D.P., Ferreira, S.T., De Felice, F.G., 2012. An anti-diabetes agent protects the mouse brain from defective insulin signaling caused by Alzheimer's disease- associated Abeta oligomers. J. Clin. Invest. 122, 1339–1353.

Brownlees, J., Irving, N.G., Brion, J.P., Gibb, B.J., Wagner, U., Woodgett, J., Miller, C.C., 1997. Tau phosphorylation in transgenic mice expressing glycogen synthase kinase-3beta transgenes. Neuroreport 8, 3251–3255.

Butterfield, D.A., Di Domenico, F., Barone, E., 2014. Elevated risk of type 2 diabetes for development of Alzheimer disease: a key role for oxidative stress in brain. Biochim. Biophys. Acta 1842, 1693–1706.

Cassano, T., Romano, A., Macheda, T., Colangeli, R., Cimmino, C.S., Petrella, A., LaFerla, F.M., Cuomo, V., Gaetani, S., 2011. Olfactory memory is impaired in a triple transgenic model of Alzheimer disease. Behav. Brain Res. 224, 408–412.

Cassano, T., Serviddio, G., Gaetani, S., Romano, A., Dipasquale, P., Cianci, S., Bellanti, F., Laconca, L., Romano, A.D., Padalino, I., LaFerla, F.M., Nicoletti, F., Cuomo, V., Vendemiale, G., 2012. Glutamatergic alterations and mitochondrial impairment in a murine model of Alzheimer disease. Neurobiol. Aging 33 (1121), e1–12.

Cenini, G., Sultana, R., Memo, M., Butterfield, D.A., 2008. Effects of oxidative and nitrosative stress in brain on p53 proapoptotic protein in amnestic mild cognitive impairment and Alzheimer disease. Free Radic. Biol. Med. 45, 81–85.

Chatterjee, S., Mudher, A., 2018. Alzheimer's Disease and Type 2 Diabetes: a critical Assessment of the Shared Pathological Traits. Front. Neurosci. 12, 383.

Cheng, C.M., Tseng, V., Wang, J., Wang, D., Matyakhina, L., Bondy, C.A., 2005. Tau is hyperphosphorylated in the insulin-like growth factor-I null brain. Endocrinology 146, 5086–5091.

Chong, Z.Z., Li, F., Maiese, K., 2005. Oxidative stress in the brain: novel cellular targets that govern survival during neurodegenerative disease. Prog. Neurobiol. 75, 207–246.

Cole, A., Frame, S., Cohen, P., 2004. Further evidence that the tyrosine phosphorylation of glycogen synthase kinase-3 (GSK3) in mammalian cells is an autophosphorylation

event. Biochem. J. 377, 249–255.
Congdon, E.E., Sigurdsson, E.M., 2018. Tau-Targeting Therapies for Alzheimer Disease. (Nat Rev Neurol).
de la Monte, S.M., 2009. Insulin resistance and Alzheimer's disease. BMB Rep. 42, 475–481.
de la Monte, S.M., Tong, M., 2014. Brain metabolic dysfunction at the core of Alzheimer's disease. Biochem. Pharmacol. 88, 548–559.
Di Domenico, F., Perluigi, M., Barone, E., 2013. Biliverdin Reductase-A correlates with inducible nitric oxide synthasein in atorvastatin treated aged canine brain. Neural Regen. Res. 8, 1925–1937.
Dixit, R., Ross, J.L., Goldman, Y.E., Holzbaur, E.L., 2008. Differential regulation of dynein and kinesin motor proteins by tau. Science 319, 1086–1089.
Doble, B.W., Woodgett, J.R., 2003. GSK-3: tricks of the trade for a multi-tasking kinase. J. Cell Sci. 116, 1175–1186.
Engel, T., Hernandez, F., Avila, J., Lucas, J.J., 2006. Full reversal of Alzheimer's disease-like phenotype in a mouse model with conditional overexpression of glycogen synthase kinase-3. J. Neurosci. 26, 5083–5090.
Farr, S.A., Ripley, J.L., Sultana, R., Zhang, Z., Niehoff, M.L., Platt, T.L., Murphy, M.P., Morley, J.E., Kumar, V., Butterfield, D.A., 2014. Antisense oligonucleotide against GSK-3beta in brain of SAMP8 mice improves learning and memory and decreases oxidative stress: Involvement of transcription factor Nrf2 and implications for Alzheimer disease. Free Radic. Biol. Med. 67, 387–395.
Frame, S., Cohen, P., 2001. GSK3 takes Centre stage more than 20 years after its discovery. Biochem. J. 359, 1–16.
Gerlier, D., Thomasset, N., 1986. Use of MTT colorimetric assay to measure cell activation. J. Immunol. Methods 94, 57–63.
Gibbs, P.E., Miralem, T., Lerner-Marmarosh, N., Tudor, C., Maines, M.D., 2012. Formation of ternary complex of human biliverdin reductase-protein kinase Cdelta-ERK2 protein is essential for ERK2-mediated activation of Elk1 protein, nuclear factor-kappaB, and inducible nitric-oxidase synthase (iNOS). J. Biol. Chem. 287, 1066–1079.
Gibbs, P.E., Lerner-Marmarosh, N., Poulin, A., Farah, E., Maines, M.D., 2014. Human biliverdin reductase-based peptides activate and inhibit glucose uptake through direct interaction with the kinase domain of insulin receptor. FASEB J. 28, 2478–2491.
Godemann, R., Biernat, J., Mandelkow, E., Mandelkow, E.M., 1999. Phosphorylation of tau protein by recombinant GSK-3beta: pronounced phosphorylation at select Ser/Thr-Pro motifs but no phosphorylation at Ser262 in the repeat domain. FEBS Lett. 454, 157–164.
Griffin, R.J., Moloney, A., Kelliher, M., Johnston, J.A., Ravid, R., Dockery, P., O'Connor, R., O'Neill, C., 2005. Activation of Akt/PKB, increased phosphorylation of Akt substrates and loss and altered distribution of Akt and PTEN are features of Alzheimer's disease pathology. J. Neurochem. 93, 105–117.
Hanger, D.P., Noble, W., 2011. Functional implications of glycogen synthase kinase-3-mediated tau phosphorylation. Int. J. Alzheimers Dis. 2011, 352805.
Harr, S.D., Hollister, R.D., Hyman, B.T., 1996. Glycogen synthase kinase 3 alpha and 3 beta do not colocalize with neurofibrillary tangles. Neurobiol. Aging 17, 343–348.
Hermida, M.A., Dinesh Kumar, J., Leslie, N.R., 2017. GSK3 and its interactions with the PI3K/AKT/mTOR signalling network. Adv Biol Regul. 65, 5–15.
Huber, C.M., Yee, C., May, T., Dhanala, A., Mitchell, C.S., 2018. Cognitive Decline in Preclinical Alzheimer's Disease: Amyloid-Beta versus Tauopathy. J. Alzheimers Dis. 61, 265–281.
Hughes, K., Nikolakaki, E., Plyte, S.E., Totty, N.F., Woodgett, J.R., 1993. Modulation of the glycogen synthase kinase-3 family by tyrosine phosphorylation. EMBO J. 12, 803–808.
Ishizawa, T., Sahara, N., Ishiguro, K., Kersh, J., McGowan, E., Lewis, J., Hutton, M., Dickson, D.W., Yen, S.H., 2003. Co-localization of glycogen synthase kinase-3 with neurofibrillary tangles and granulovacuolar degeneration in transgenic mice. Am. J. Pathol. 163, 1057–1067.
Jensen, J., Brennesvik, E.O., Lai, Y.C., Shepherd, P.R., 2007. GSK-3beta regulation in skeletal muscles by adrenaline and insulin: evidence that PKA and PKB regulate different pools of GSK-3. Cell. Signal. 19, 204–210.
Jope, R.S., Johnson, G.V., 2004. The glamour and gloom of glycogen synthase kinase-3. Trends Biochem. Sci. 29, 95–102.
Kapitulnik, J., Maines, M.D., 2009. Pleiotropic functions of biliverdin reductase: cellular signaling and generation of cytoprotective and cytotoxic bilirubin. Trends Pharmacol. Sci. 30, 129–137.
Krishnankutty, A., Kimura, T., Saito, T., Aoyagi, K., Asada, A., Takahashi, S.I., Ando, K., Ohara-Imaizumi, M., Ishiguro, K., Hisanaga, S.I., 2017. In vivo regulation of glycogen synthase kinase 3beta activity in neurons and brains. Sci. Rep. 7, 8602.
Lebouvier, T., Pasquier, F., Buee, L., 2017. Update on tauopathies. Curr. Opin. Neurol 30, 589–598.
Lee, V.M., Goedert, M., Trojanowski, J.Q., 2001. Neurodegenerative tauopathies. Annu. Rev. Neurosci. 24, 1121–1159.
Lerner-Marmarosh, N., Shen, J., Torno, M.D., Kravets, A., Hu, Z., Maines, M.D., 2005. Human biliverdin reductase: a member of the insulin receptor substrate family with serine/threonine/tyrosine kinase activity. Proc. Natl. Acad. Sci. U. S. A. 102, 7109–7114.
Lerner-Marmarosh, N., Miralem, T., Gibbs, P.E., Maines, M.D., 2008. Human biliverdin reductase is an ERK activator; hBVR is an ERK nuclear transporter and is required for MAPK signaling. Proc. Natl. Acad. Sci. U. S. A. 105, 6870–6875.
Leroy, A., Landrieu, I., Huvent, I., Legrand, D., Codeville, B., Wieruszeski, J.M., Lippens, G., 2010. Spectroscopic studies of GSK3{beta} phosphorylation of the neuronal tau protein and its interaction with the N-terminal domain of apolipoprotein E. J. Biol. Chem. 285, 33435–33444.
Liu, S.J., Zhang, J.Y., Li, H.L., Fang, Z.Y., Wang, Q., Deng, H.M., Gong, C.X., Grundke-Iqbal, I., Iqbal, K., Wang, J.Z., 2004. Tau becomes a more favorable substrate for GSK-3 when it is prephosphorylated by PKA in rat brain. J. Biol. Chem. 279, 50078–50088.
Llorens-Martin, M., Jurado, J., Hernandez, F., Avila, J., 2014. GSK-3beta, a pivotal kinase in Alzheimer disease. Front. Mol. Neurosci. 7, 46.
Lochhead, P.A., Kinstrie, R., Sibbet, G., Rawjee, T., Morrice, N., Cleghon, V., 2006. A chaperone-dependent GSK3beta transitional intermediate mediates activation-loop autophosphorylation. Mol. Cell 24, 627–633.
Lovestone, S., Hartley, C.L., Pearce, J., Anderton, B.H., 1996. Phosphorylation of tau by glycogen synthase kinase-3 beta in intact mammalian cells: the effects on the organization and stability of microtubules. Neuroscience 73, 1145–1157.
Lucas, J.J., Hernandez, F., Gomez-Ramos, P., Moran, M.A., Hen, R., Avila, J., 2001. Decreased nuclear beta-catenin, tau hyperphosphorylation and neurodegeneration in GSK-3beta conditional transgenic mice. EMBO J. 20, 27–39.
Mancuso, C., Barone, E., Guido, P., Miceli, F., Di Domenico, F., Perluigi, M., Santangelo, R., Preziosi, P., 2012. Inhibition of lipid peroxidation and protein oxidation by endogenous and exogenous antioxidants in rat brain microsomes in vitro. Neurosci. Lett. 518, 101–105.
Mandelkow, E.M., Drewes, G., Biernat, J., Gustke, N., Van Lint, J., Vandenheede, J.R., Mandelkow, E., 1992. Glycogen synthase kinase-3 and the Alzheimer-like state of microtubule-associated protein tau. FEBS Lett. 314, 315–321.
Manning, B.D., Toker, A., 2017. AKT/PKB Signaling: Navigating the Network. Cell 169, 381–405.
Medina, M., Garrido, J.J., Wandosell, F.G., 2011. Modulation of GSK-3 as a Therapeutic Strategy on Tau Pathologies. Front. Mol. Neurosci. 4, 24.
Miralem, T., Lerner-Marmarosh, N., Gibbs, P.E., Jenkins, J.L., Heimiller, C., Maines, M.D., 2016. Interaction of human biliverdin reductase with Akt/protein kinase B and phosphatidylinositol-dependent kinase 1 regulates glycogen synthase kinase 3 activity: a novel mechanism of Akt activation. FASEB J. 30, 2926–2944.
Morales-Corraliza, J., Wong, H., Mazzella, M.J., Che, S., Lee, S.H., Petkova, E., Wagner, J.D., Hemby, S.E., Ginsberg, S.D., Mathews, P.M., 2016. Brain-Wide Insulin Resistance, Tau Phosphorylation changes, and Hippocampal Neprilysin and Amyloid-beta Alterations in a Monkey Model of Type 1 Diabetes. J. Neurosci. 36, 4248–4258.
Neumann, K.F., Rojo, L., Navarrete, L.P., Farias, G., Reyes, P., Maccioni, R.B., 2008. Insulin resistance and Alzheimer's disease: molecular links & clinical implications. Curr. Alzheimer Res. 5, 438–447.
Nicolia, V., Ciraci, V., Cavallaro, R.A., Ferrer, I., Scarpa, S., Fuso, A., 2017. GSK3beta 5′-flanking DNA Methylation and Expression in Alzheimer's Disease patients. Curr. Alzheimer Res. 14, 753–759.
Oddo, S., Caccamo, A., Shepherd, J.D., Murphy, M.P., Golde, T.E., Kayed, R., Metherate, R., Mattson, M.P., Akbari, Y., LaFerla, F.M., 2003. Triple-transgenic model of Alzheimer's disease with plaques and tangles: intracellular Abeta and synaptic dysfunction. Neuron 39, 409–421.
Pei, J.J., Tanaka, T., Tung, Y.C., Braak, E., Iqbal, K., Grundke-Iqbal, I., 1997. Distribution, levels, and activity of glycogen synthase kinase-3 in the Alzheimer disease brain. J. Neuropathol. Exp. Neurol. 56, 70–78.
Pei, J.J., Braak, E., Braak, H., Grundke-Iqbal, I., Iqbal, K., Winblad, B., Cowburn, R.F., 1999. Distribution of active glycogen synthase kinase 3beta (GSK-3beta) in brains staged for Alzheimer disease neurofibrillary changes. J. Neuropathol. Exp. Neurol. 58, 1010–1019.
Pei, J.J., Khatoon, S., An, W.L., Nordlinder, M., Tanaka, T., Braak, H., Tsujio, I., Takeda, M., Alafuzoff, I., Winblad, B., Cowburn, R.F., Grundke-Iqbal, I., Iqbal, K., 2003. Role of protein kinase B in Alzheimer's neurofibrillary pathology. Acta Neuropathol. 105, 381–392.
Perluigi, M., De Marco, F., Foppoli, C., Coccia, R., Blarzino, C., Marcante, M.L., Cini, C., 2003. Tyrosinase protects human melanocytes from ROS-generating compounds. Biochem. Biophys. Res. Commun. 305, 250–256.
Petersen, R.C., 2003. Mild cognitive impairment clinical trials. Nat. Rev. Drug Discov. 2, 646–653.
Rivera, E.J., Goldin, A., Fulmer, N., Tavares, R., Wands, J.R., de la Monte, S.M., 2005. Insulin and insulin-like growth factor expression and function deteriorate with progression of Alzheimer's disease: link to brain reductions in acetylcholine. J. Alzheimers Dis. 8, 247–268.
Rockenstein, E., Torrance, M., Adame, A., Mante, M., Bar-on, P., Rose, J.B., Crews, L., Masliah, E., 2007. Neuroprotective effects of regulators of the glycogen synthase kinase-3beta signaling pathway in a transgenic model of Alzheimer's disease are associated with reduced amyloid precursor protein phosphorylation. J. Neurosci. 27, 1981–1991.
Sajan, M., Hansen, B., Ivey 3rd, R., Sajan, J., Ari, C., Song, S., Braun, U., Leitges, M., Farese-Higgs, M., Farese, R.V., 2016. Brain insulin signaling is increased in insulin-resistant states and decreases in FOXOs and PGC-1alpha and increases in Abeta1-40/42 and Phospho-Tau May Abet Alzheimer Development. Diabetes 65, 1892–1903.
Salim, M., Brown-Kipphut, B.A., Maines, M.D., 2001. Human biliverdin reductase is autophosphorylated, and phosphorylation is required for bilirubin formation. J. Biol. Chem. 276, 10929–10934.
Schubert, M., Brazil, D.P., Burks, D.J., Kushner, J.A., Ye, J., Flint, C.L., Farhang-Fallah, J., Dikkes, P., Warot, X.M., Rio, C., Corfas, G., White, M.F., 2003. Insulin receptor substrate-2 deficiency impairs brain growth and promotes tau phosphorylation. J. Neurosci. 23, 7084–7092.
Schubert, M., Gautam, D., Surjo, D., Ueki, K., Baudler, S., Schubert, D., Kondo, T., Alber, J., Galldiks, N., Kustermann, E., Arndt, S., Jacobs, A.H., Krone, W., Kahn, C.R., Bruning, J.C., 2004. Role for neuronal insulin resistance in neurodegenerative diseases. Proc. Natl. Acad. Sci. U. S. A. 101, 3100–3105.
Shin, S.Y., Kim, C.G., Jho, E.H., Rho, M.S., Kim, Y.S., Kim, Y.H., Lee, Y.H., 2004. Hydrogen peroxide negatively modulates Wnt signaling through downregulation of beta-catenin. Cancer Lett. 212, 225–231.
Shiurba, R.A., Ishiguro, K., Takahashi, M., Sato, K., Spooner, E.T., Mercken, M., Yoshida,

R., Wheelock, T.R., Yanagawa, H., Imahori, K., Nixon, R.A., 1996. Immunocytochemistry of tau phosphoserine 413 and tau protein kinase I in Alzheimer pathology. Brain Res. 737, 119–132.
Steen, E., Terry, B.M., Rivera, E.J., Cannon, J.L., Neely, T.R., Tavares, R., Xu, X.J., Wands, J.R., de la Monte, S.M., 2005. Impaired insulin and insulin-like growth factor expression and signaling mechanisms in Alzheimer's disease–is this type 3 diabetes? J. Alzheimers Dis. 7, 63–80.
Sultana, R., Perluigi, M., Newman, S.F., Pierce, W.M., Cini, C., Coccia, R., Butterfield, D.A., 2010. Redox proteomic analysis of carbonylated brain proteins in mild cognitive impairment and early Alzheimer's disease. Antioxid. Redox Signal. 12, 327–336.
Sun, W., Qureshi, H.Y., Cafferty, P.W., Sobue, K., Agarwal-Mawal, A., Neufield, K.D., Paudel, H.K., 2002. Glycogen synthase kinase-3beta is complexed with tau protein in brain microtubules. J. Biol. Chem. 277, 11933–11940.
Sutherland, C., Leighton, I.A., Cohen, P., 1993. Inactivation of glycogen synthase kinase-3 beta by phosphorylation: new kinase connections in insulin and growth-factor signalling. Biochem. J. 296 (Pt 1), 15–19.
Talbot, K., Wang, H.Y., Kazi, H., Han, L.Y., Bakshi, K.P., Stucky, A., Fuino, R.L., Kawaguchi, K.R., Samoyedny, A.J., Wilson, R.S., Arvanitakis, Z., Schneider, J.A., Wolf, B.A., Bennett, D.A., Trojanowski, J.Q., Arnold, S.E., 2012. Demonstrated brain insulin resistance in Alzheimer's disease patients is associated with IGF-1 resistance, IRS-1 dysregulation, and cognitive decline. J. Clin. Invest. 122, 1316–1338.
Tramutola, A., Triplett, J.C., Di Domenico, F., Niedowicz, D.M., Murphy, M.P., Coccia, R., Perluigi, M., Butterfield, D.A., 2015. Alteration of mTOR signaling occurs early in the progression of Alzheimer disease (AD): analysis of brain from subjects with pre-clinical AD, amnestic mild cognitive impairment and late-stage AD. J. Neurochem. 133, 739–749.
Triani, F., Tramutola, A., Di Domenico, F., Sharma, N., Butterfield, D.A., Head, E., Perluigi, M., Barone, E., 2018 Oct. Biliverdin reductase-A impairment links brain insulin resistance with increased Abeta production in an animal model of aging: Implications for Alzheimer disease. Biochim. Biophys. Acta 1864 (10), 3181–3194. https://doi.org/10.1016/j.bbadis.2018.07.005.
van der Harg, J.M., Eggels, L., Bangel, F.N., Ruigrok, S.R., Zwart, R., Hoozemans, J.J.M., la Fleur, S.E., Scheper, W., 2017. Insulin deficiency results in reversible protein kinase A activation and tau phosphorylation. Neurobiol. Dis. 103, 163–173.
Vershinin, M., Carter, B.C., Razafsky, D.S., King, S.J., Gross, S.P., 2007. Multiple-motor based transport and its regulation by Tau. Proc. Natl. Acad. Sci. U. S. A. 104, 87–92.
Wang, Y., Mandelkow, E., 2016. Tau in physiology and pathology. Nat. Rev. Neurosci. 17, 5–21.
Yarchoan, M., Toledo, J.B., Lee, E.B., Arvanitakis, Z., Kazi, H., Han, L.Y., Louneva, N., Lee, V.M., Kim, S.F., Trojanowski, J.Q., Arnold, S.E., 2014. Abnormal serine phosphorylation of insulin receptor substrate 1 is associated with tau pathology in Alzheimer's disease and tauopathies. Acta Neuropathol. 128, 679–689.
Zhang, X., Tang, S., Zhang, Q., Shao, W., Han, X., Wang, Y., Du, Y., 2016. Endoplasmic reticulum stress mediates JNK-dependent IRS-1 serine phosphorylation and results in Tau hyperphosphorylation in amyloid beta oligomer-treated PC12 cells and primary neurons. Gene 587, 183–193.
Zhang, Y., Huang, N.Q., Yan, F., Jin, H., Zhou, S.Y., Shi, J.S., Jin, F., 2018. Diabetes mellitus and Alzheimer's disease: GSK-3beta as a potential link. Behav. Brain Res. 339, 57–65.